scientific reports

Check for updates

OPEN

Resource prioritization and balancing for the quantum internet

Laszlo Gyongyosi[1,2]✉ & Sandor Imre[1]

The quantum Internet enables networking based on the fundamentals of quantum mechanics. Here, methods and procedures of resource prioritization and resource balancing are defined for the quantum Internet. We define a model for resource consumption optimization in quantum repeaters, and a strongly-entangled network structure for resource balancing. We study the resource-balancing efficiency of the strongly-entangled structure. We prove that a strongly-entangled quantum network is two times more efficient in a resource balancing problem than a full-mesh network of the traditional Internet.

The quantum Internet[1–30] aims to provide an adequate answer to the computational power that becomes available with quantum computers[31–60]. To provide a seamless transition to the legal users from the traditional Internet to the quantum Internet, the creation of advanced services and methods for the quantum Internet are emerging tasks[52–54,61–67]. The quantum Internet is modeled as a quantum network consisting of quantum repeaters and entangled connections between the quantum repeaters[2,66–129]. This entangled quantum network forms a general framework for the quantum Internet, enabling long-distance quantum communications, multi-hop entanglement and multi-hop QKD (quantum key distribution)[25], utilization of quantum protocols, advanced distributed computing, high-precision sensor networks, and the establishment of a global-scale quantum Internet.

A crucial problem related to the quantum Internet is the resource optimization of the quantum repeaters and the handling of resource requirement issues such as non-servable resource requests in the quantum repeaters[18–26]. These fundamental questions are still open and have not been addressed for the quantum Internet.

Here, we define methods for resource prioritization and resource balancing for the quantum Internet. The aim of the proposed solutions is to optimize the resource allocation mechanisms and to reduce the resource consumption of the network entities of the quantum Internet. A model of resource consumption[130–134] of quantum repeaters is proposed, and its optimization is realized through the weightings of the entanglement throughputs of the entangled connections of the quantum repeaters. We also propose a method for optimizing the entanglement swapping procedure and determine the conditions of deadlock-free entanglement swapping. For resource balancing, a strongly-entangled network structure is defined. This network is modeled as an independent entity in the quantum Internet, composed of an arbitrary number of quantum repeaters such that all quantum repeaters are entangled with each other. The primary aim of the strongly-entangled structure is to serve those quantum nodes that have non-servable resource requests due to resource issues or an arbitrary network issue; these quantum nodes are referred to as low-priority quantum nodes.

The strongly-entangled structure injects additional resources into the quantum network to manage the resource issues of an arbitrary number of low-priority quantum nodes. The structure also provides optimized resource balancing for the low-priority quantum nodes. We prove the resource-balancing efficiency of the strongly-entangled structure and study its fault tolerance. We show that a strongly-entangled quantum network structure, due to the advanced attributes of quantum networking, is two times more efficient in resource balancing than a classical full-mesh[135,136] network structure.

The novel contributions of our manuscript are as follows:

1. We define methods and procedures for resource prioritization and resource balancing in the quantum Internet.

[1]Department of Networked Systems and Services, Budapest University of Technology and Economics, Budapest 1117, Hungary. [2]MTA-BME Information Systems Research Group, Hungarian Academy of Sciences, Budapest 1051, Hungary. ✉email: gyongyosi@hit.bme.hu

2. The resource prioritization covers the resource consumption optimization of the quantum repeaters via the entanglement throughput weightings, prioritization of entanglement swapping in the quantum repeaters, and deadlock-free entanglement swapping.
3. A strongly-entangled structure is defined for an optimal resource balancing. We prove the resource-balancing efficiency of the proposed structure and prove its fault tolerance. We show that a strongly-entangled quantum network structure is two times more efficient in resource balancing than a classical full-mesh network structure.

This paper is organized as follows. In "Preliminaries" section, preliminaries are summarized. In "Method" section, methods for resource consumption optimization are defined. "Strongly-entangled structure for resource balancing in the quantum internet" section proposes a solution for optimal resource balancing. A performance analysis is given in "Performance evaluation" section. Finally, "Conclusions" section provides the conclusions. Supplementary information is included in the Appendix.

Preliminaries

Basic terms. *Entanglement fidelity.* The aim of the entanglement distribution procedure is to establish a d-dimensional entangled system between the distant points A and B, through the intermediate quantum repeater nodes. Let $d = 2$, and let $|\beta_{00}\rangle = \frac{1}{\sqrt{2}}(|00\rangle + |11\rangle)$ be the entangled state subject to be established between distant points A and B. At a particular two-partite state σ established between A and B, the fidelity of σ is evaluated as

$$F = \langle\beta_{00}|\sigma|\beta_{00}\rangle. \tag{1}$$

Without loss of generality, an aim of a practical entanglement distribution is to reach $F \geq 0.98$[2–4,12,68,69,137,138].

Entangled network structure. Let V refer to the nodes of an entangled quantum network N, which consists of a transmitter node $A \in V$, a receiver node $B \in V$, and quantum repeater nodes $R_i \in V$, $i = 1, \ldots, q$. Let $E = \{E_j\}$, $j = 1, \ldots, m$ refer to a set of edges (an edge refers to an entangled connection in a graph representation) between the nodes of V, where each E_j identifies an L_l-level entanglement, $l = 1, \ldots, r$, between quantum nodes x_j and y_j of edge E_j, respectively. Let $N = (V, \mathscr{S})$ be an actual quantum network with $|V|$ nodes and a set $\mathscr{S}$ of entangled connections. An L_l-level, $l = 1, \ldots, r$, entangled connection $E_{\mathrm{L}_l}(x, y)$, refers to the shared entanglement between a source node x and a target node y, with hop-distance

$$d(x, y)_{\mathrm{L}_l} = 2^{l-1}, \tag{2}$$

since the entanglement swapping (extension) procedure doubles the span of the entangled pair in each step. This architecture is also referred to as the doubling architecture[2,68,69,138].

For a particular L_l-level entangled connection $E_{\mathrm{L}_l}(x, y)$ with hop-distance (2), there are $d(x, y)_{\mathrm{L}_l} - 1$ intermediate nodes between the quantum nodes x and y.

Entanglement throughput. Let $B_F(E^i_{\mathrm{L}_l})$ refer to the entanglement throughput of a given L_l entangled connection $E^i_{\mathrm{L}_l}$ measured in the number of d-dimensional entangled states established over $E^i_{\mathrm{L}_l}$ per sec at a particular fidelity F (dimension of a qubit system is $d = 2$)[2–4,12,68,69,137,138].

For any entangled connection $E^i_{\mathrm{L}_l}$, a condition c should be satisfied, as

$$c : B_F(E^i_{\mathrm{L}_l}) \geq B^*_F(E^i_{\mathrm{L}_l}), \text{ for } \forall i, \tag{3}$$

where $B^*_F(E^i_{\mathrm{L}_l})$ is a critical lower bound on the entanglement throughput at a particular fidelity F of a given $E^i_{\mathrm{L}_l}$, i.e., $B_F(E^i_{\mathrm{L}_l})$ of a particular $E^i_{\mathrm{L}_l}$ has to be at least $B^*_F(E^i_{\mathrm{L}_l})$.

Oscillator cycles. To quantify the entanglement throughput of the entangled connections, time is measured in number of cycles C. The time t_C of a cycle C is determined by an oscillator unit O_C that is available for all the entities of the quantum network, such that $t_C = 1/f_C$, where f_C is the frequency of O_C, with $f_C = 1/t_C$.

Definitions. *Resource consumption of a quantum repeater.* Let $\alpha(R_i, \mathrm{L}_l(k))$ be the resource consumption of quantum repeater R_i associated with a k-th entangled connection $\mathrm{L}_l(k)$, $k = 1, \ldots, z$, where l is the level of entanglement of the connection and z is the total number of entangled connections of R_i.

Let $\Upsilon(R_i, \mathrm{L}_l(k))$ be the resource consumption of quantum repeater R_i associated with the quantum memory usage at $\mathrm{L}_l(k)$; let $\phi(R_i, \mathrm{L}_l(k))$ be the resource consumption of quantum repeater R_i associated with the entanglement purification of $\mathrm{L}_l(k)$; let $\tau(R_i, \mathrm{L}_l(k))$ be the resource consumption of quantum repeater R_i associated with the entanglement distribution to a target node B; and let $\nu(R_i, \mathrm{L}_l(k))$ be the resource consumption of quantum repeater R_i associated with the entanglement swapping U_S of $\mathrm{L}_l(k)$. Then, $\alpha(R_i, \mathrm{L}_l(k))$ can be defined as

$$\alpha(R_i, \mathrm{L}_l(k)) := B_F(\mathrm{L}_l(k))(\partial(R_i, \mathrm{L}_l(k))) + \zeta(R_i, \mathrm{L}_l(k)) + C(R_i, \mathrm{L}_l(k)), \tag{4}$$

where the term $\partial(R_i, \mathrm{L}_l(k))$ is defined as

$$\partial(R_i, \mathrm{L}_l(k)) := \Upsilon(R_i, \mathrm{L}_l(k)) + \phi(R_i, \mathrm{L}_l(k)) + \tau(R_i, \mathrm{L}_l(k)) + \nu(R_i, \mathrm{L}_l(k)), \tag{5}$$

where $B_F(\mathrm{L}_l(k))$ is the entanglement throughput (Bell states per C) of the entangled connection $\mathrm{L}_l(k)$, while $\zeta(R_i, \mathrm{L}_l(k))$ identifies the resource consumption of quantum repeater R_i associated with the path selection, and $C(R_i, \mathrm{L}_l(k))$ refers to the cost of auxiliary classical communications.

Set of outcoming entangled states. Let ρ_A be an input entangled density matrix (i.e., half pair of an entangled state) in quantum repeater R_i, and let $\mathscr{A}(\rho_A)$ be the set of possible r outcoming entangled states in R_i,

$$\mathscr{A}(\rho_A) := \{\sigma_{B,1}, \ldots, \sigma_{B,r}\}, \tag{6}$$

where $\sigma_{B,i}$ is the i-th possible outcoming density matrix. The set $\mathscr{A}(\rho_A)$ is therefore identifies those (purified) entangled states, that can be selected for the U_S entanglement swapping with ρ_A to formulate an extended entangled connection via R_i.

Extended entangled connection. Using (6), an extended entangled connection is depicted as

$$\mathrm{L}_l(R_s(\beta(\rho_A)), R_d(\beta(\sigma_B))), \tag{7}$$

where $\beta(\rho_A)$ identifies subsystem ρ_A of the entangled state β_{AB}, $\beta(\sigma_B)$ identifies subsystem σ_B of the entangled state β_{AB}, $R_s(\beta(\rho_A))$ is the R_s source quantum node with $\beta(\rho_A)$, while $R_d(\beta(\sigma_B))$ is the R_d destination quantum node with $\beta(\sigma_B)$, where $\beta(\sigma_B)$ is selected from set $\mathscr{A}(\rho_A)$ for the entanglement swapping to formulate β_{AB}.

Set of destination quantum nodes. The set $\mathscr{A}(\rho_A)$ in (6) is determined for a particular incoming density ρ_A by the set $\mathscr{D}(R_i)$ of R_d destination quantum nodes that share an entangled connection with a current quantum repeater R_i, as

$$\mathscr{D}(R_i) := \{R_d(\beta(\sigma_{B,1})), \ldots, R_d(\beta(\sigma_{B,r}))\}, \tag{8}$$

where $R_d(\beta(\sigma_{B,i}))$ refers to the R_d destination quantum node with $\beta(\sigma_{B,i}), i = 1, \ldots, r$.

Set of entangled connections via swapping. Let $\mathscr{S}_{\mathscr{P}}(R_i, \rho_A)$ refer to the set of entangled connections that contains the entangled connection that is resulted between distant source R_s and destination R_d via an entanglement swapping in a particular quantum repeater R_i using input state ρ_A and output state σ_B, as

$$\mathscr{S}_{\mathscr{P}}(R_i, \rho_A) := \mathscr{S}_{\mathscr{P}}(\sigma_B, R_s(\beta(\rho_A)), R_d(\beta(\sigma_B))) \subseteq \mathscr{S}_{\mathscr{P}}(R_i, R_d(\beta(\sigma_B))), \tag{9}$$

where $\mathscr{S}_{\mathscr{P}}(R_i, R_d(\sigma_B))$ is the set of paths that pass through R_i using the entangled pair $\beta(\sigma_B)$ in R_d.

Strongly-entangled structure. For a $\mathscr{S}_{\mathscr{N}}$ strongly-entangled structure, the number of low-priority quantum nodes (quantum nodes with non-servable resource requests) in N is n_c, while $|\mathscr{S}_{\mathscr{N}}|$ is the number of quantum repeaters in a $\mathscr{S}_{\mathscr{N}}$ strongly-entangled structure, $R_1^{(\mathscr{S}_{\mathscr{N}})}, \ldots, R_{|\mathscr{S}_{\mathscr{N}}|}^{(\mathscr{S}_{\mathscr{N}})}$. Since $\mathscr{S}_{\mathscr{N}}$ is strongly-entangled, each quantum repeater in $\mathscr{S}_{\mathscr{N}}$ has $|\mathscr{S}_{\mathscr{N}}| - 1$ entangled connections, and the $|E(\mathscr{S}_{\mathscr{N}})|$ number of entangled connections within $\mathscr{S}_{\mathscr{N}}$ is

$$|E(\mathscr{S}_{\mathscr{N}})| := \frac{|\mathscr{S}_{\mathscr{N}}| \cdot (|\mathscr{S}_{\mathscr{N}}| - 1)}{2}. \tag{10}$$

The entanglement levels of the $|E(\mathscr{S}_{\mathscr{N}})|$ entangled connections in $\mathscr{S}_{\mathscr{N}}$ are defined in the following manner. Let A be the ingress node of $\mathscr{S}_{\mathscr{N}}$, and let B be the egress node of $\mathscr{S}_{\mathscr{N}}$, with hop-distance $d(A, B)$. Then, the $L(d(x, y))$ entangled connections in function of the $d(x, y))$ hop-distance between quantum nodes $\{x, y\} \in \mathscr{S}_{\mathscr{N}}$ in the $\mathscr{S}_{\mathscr{N}}$ strongly-entangled structure are distributed as follows:

$$L(d(x,y)) := \begin{cases} |L(1)| = |\mathscr{S}_{\mathscr{N}}| - 1 = d(A,B) \\ |L(2)| = |L(1)| - 1 \\ \vdots \\ |L(|\mathscr{S}_{\mathscr{N}}| - 2)| = |L(|\mathscr{S}_{\mathscr{N}}| - 3)| - 1 \\ |L(|\mathscr{S}_{\mathscr{N}}|) - 1| = L(d(A,B)) = 1 \end{cases}, \tag{11}$$

at a particular number $|\mathscr{S}_{\mathscr{N}}|$ of quantum nodes. (Note, the strongly-entangled structure utilizes different entanglement levels than the doubling architecture, therefore in (11) the entanglement levels are denoted in different manner.)

Capability of a strongly-entangled structure. Assuming that there is a set $\mathscr{S}_{n_c}$ of n_c low-priority R_i quantum repeaters in the network, $i = 1, \ldots, n_c$, the $R_q^{(\mathscr{S}_{\mathscr{N}})}$ in $\mathscr{S}_{\mathscr{N}}$ is associated with entanglement throughput request (Bell states per C)

$$B\left(R_q^{\left(\mathscr{S}_{\mathscr{N}}\right)}, \mathscr{S}_{n_c}\right) := \frac{1}{\left|\mathscr{S}_{\mathscr{N}}\right|}\left(\sum_{i=1}^{n_c} B(R_i)\right), \tag{12}$$

while for the internal entangled connections

$$Q\left(R_q^{\left(\mathscr{S}_{\mathscr{N}}\right)}, R_z^{\left(\mathscr{S}_{\mathscr{N}}\right)}\right) := \frac{1}{\left|\mathscr{S}_{\mathscr{N}}\right|^2}\left(\sum_{i=1}^{n_c} B(R_i)\right). \tag{13}$$

where $R_z^{\left(\mathscr{S}_{\mathscr{N}}\right)}$ is a neighbor of $R_q^{\left(\mathscr{S}_{\mathscr{N}}\right)}$ in $\mathscr{S}_{\mathscr{N}}$, $z \neq q, q = 1, \ldots, \left|\mathscr{S}_{\mathscr{N}}\right|$.

Since, by definition, $R_q^{\left(\mathscr{S}_{\mathscr{N}}\right)}$ has $\left|\mathscr{S}_{\mathscr{N}}\right| - 1$ entangled connections in $\mathscr{S}_{\mathscr{N}}$, it follows that the $W\left(R_q^{\left(\mathscr{S}_{\mathscr{N}}\right)}\right)$ total entanglement throughput associated with $R_q^{\left(\mathscr{S}_{\mathscr{N}}\right)}$ within the structure of $\mathscr{S}_{\mathscr{N}}$ (Bell states per C) is as

$$\begin{aligned} W\left(R_q^{\left(\mathscr{S}_{\mathscr{N}}\right)}\right) &:= \sum_{(q,z):z\neq q} Q\left(R_q^{\left(\mathscr{S}_{\mathscr{N}}\right)}, R_z^{\left(\mathscr{S}_{\mathscr{N}}\right)}\right) \\ &= \left(\left|\mathscr{S}_{\mathscr{N}}\right| - 1\right)\frac{1}{\left|\mathscr{S}_{\mathscr{N}}\right|} B\left(R_q^{\left(\mathscr{S}_{\mathscr{N}}\right)}, \mathscr{S}_{n_c}\right) \\ &= \left(\left|\mathscr{S}_{\mathscr{N}}\right| - 1\right)\frac{1}{\left|\mathscr{S}_{\mathscr{N}}\right|^2}\left(\sum_{i=1}^{n_c} B(R_i)\right). \end{aligned} \tag{14}$$

Since there are $\left|\mathscr{S}_{\mathscr{N}}\right|$ quantum repeaters in $\mathscr{S}_{\mathscr{N}}$, the $Z\left(\mathscr{S}_{\mathscr{N}}\right)$ cumulated entanglement throughput of the quantum repeaters of $\mathscr{S}_{\mathscr{N}}$ (Bell states per C) is as

$$\begin{aligned} Z\left(\mathscr{S}_{\mathscr{N}}\right) &:= \sum_{q=1}^{\left|\mathscr{S}_{\mathscr{N}}\right|} W\left(R_q^{\left(\mathscr{S}_{\mathscr{N}}\right)}\right) \\ &= \sum_{q=1}^{\left|\mathscr{S}_{\mathscr{N}}\right|} \sum_{(q,z):z\neq q} Q\left(R_q^{\left(\mathscr{S}_{\mathscr{N}}\right)}, R_z^{\left(\mathscr{S}_{\mathscr{N}}\right)}\right) \\ &= \sum_{q=1}^{\left|\mathscr{S}_{\mathscr{N}}\right|} \left(\left|\mathscr{S}_{\mathscr{N}}\right| - 1\right)\frac{1}{\left|\mathscr{S}_{\mathscr{N}}\right|} B\left(R_q^{\left(\mathscr{S}_{\mathscr{N}}\right)}, \mathscr{S}_{n_c}\right) \\ &= \left|\mathscr{S}_{\mathscr{N}}\right|\left(\left|\mathscr{S}_{\mathscr{N}}\right| - 1\right)\frac{1}{\left|\mathscr{S}_{\mathscr{N}}\right|} B\left(R_q^{\left(\mathscr{S}_{\mathscr{N}}\right)}, \mathscr{S}_{n_c}\right) \\ &= \left|\mathscr{S}_{\mathscr{N}}\right|\left(\left|\mathscr{S}_{\mathscr{N}}\right| - 1\right)\frac{1}{\left|\mathscr{S}_{\mathscr{N}}\right|^2}\left(\sum_{i=1}^{n_c} B(R_i)\right) \\ &= \left(\left|\mathscr{S}_{\mathscr{N}}\right| - 1\right)\frac{1}{\left|\mathscr{S}_{\mathscr{N}}\right|}\left(\sum_{i=1}^{n_c} B(R_i)\right). \end{aligned} \tag{15}$$

Because of the $\mathscr{S}_{\mathscr{N}}$ strongly-entangled structure has $\left|\mathscr{S}_{\mathscr{N}}\right|\left(\left|\mathscr{S}_{\mathscr{N}}\right| - 1\right)/2$ entangled connections, the $T\left(\mathscr{S}_{\mathscr{N}}\right)$ total entanglement throughput of the entangled connections of $\mathscr{S}_{\mathscr{N}}$ (Bell states per C) is as

$$\begin{aligned} T\left(\mathscr{S}_{\mathscr{N}}\right) &:= \left|\mathscr{S}_{\mathscr{N}}\right|\left(\frac{\left|\mathscr{S}_{\mathscr{N}}\right|-1}{2}\right)\frac{1}{\left|\mathscr{S}_{\mathscr{N}}\right|^2}\left(\sum_{i=1}^{n_c} B(R_i)\right) \\ &= \left(\frac{\left|\mathscr{S}_{\mathscr{N}}\right|-1}{2}\right)\frac{1}{\left|\mathscr{S}_{\mathscr{N}}\right|}\left(\sum_{i=1}^{n_c} B(R_i)\right). \end{aligned} \tag{16}$$

Related works

In this section the related works are given.

On the problem of resource allocation and routing in quantum networks, we suggest the works of[62,70,71]. In[70], the authors study the problem of entanglement routing in practical quantum networks with limited quantum processing capabilities and with noisy optical links. The authors study how a practical quantum network can distribute high-rate entanglement simultaneously between multiple pairs of users. In[71], the authors study new

routing algorithms for a quantum network with noisy quantum devices such that each can store a small number of qubits. In[62], the problem of entanglement generation is modeled through a stochastic framework that takes into consideration the key physical-layer mechanisms affecting the end-to-end entanglement rate. The author derives the closed-form expression of the end-to-end entanglement rate for an arbitrary path, and design a routing protocol for quantum networks.

In a quantum Internet scenario, the entanglement purification is a procedure that takes two imperfect systems σ_1 and σ_2 with initial fidelity $F_0 < 1$, and outputs a higher-fidelity density ρ such that $F(\rho) > F_0$. In[139], the authors propose novel physical approaches to assess and optimize entanglement purification schemes. The proposed solutions provide an optimization framework of practical entanglement purification.

In[140], a satellite-to-ground QKD system has been demonstrated. In[141], the authors demonstrated the quantum teleportation of independent single-photon qubits. In[142], the authors demonstrated the Bell inequality violation using electron spins. In[143], the authors demonstrated modular entanglement of atomic qubits using photons and phonons. For an experimental realization of quantum repeaters based on atomic ensembles and linear optics, see[144,145].

Since quantum channels also have a fundamental role in the quantum Internet, we suggest the review paper of[137], for some specialized applications of quantum channels. For a review on some recent results of quantum computing technology, we suggest[146]. For some recent services developed for the quantum Internet, we suggest[12–17,27–29].

Some other related topics are as follows. The works[12–14,68,69,137,138] are related to the utilization of entanglement for long-distance quantum communications and for a global-scale quantum Internet, and also to the various aspects of quantum networks in a quantum Internet setting[137,147–155].

A technical roadmap on the experimental development of the quantum Internet has been provided in[20], see also[156]. For some important works on the experimental implementations, we suggest[157–180].

Method

Resource consumption optimization via entanglement throughput prioritization. The aim of the entanglement throughput prioritization is to find an optimal distribution of the entanglement throughputs of the entangled connections of a given quantum repeater. The prioritization leads to an optimized, nearly uniform distribution of the resource consumptions of the quantum repeaters.

Theorem 1 (Resource consumption of a quantum repeater). *The $\mathscr{C}(R_i)$ resource consumption of a quantum repeater R_i is adjustable by distributing the weight coefficients associated with the entanglement throughputs of the entangled connections of R_i.*

Proof Let us assume that there are a source node A and a destination node B in the network.

Assuming that the total number of the (logical) incoming entangled connections $\mathrm{L}_l(k)$ of quantum repeater R_i is z, the total resource consumption $\mathscr{C}(R_i)$ of quantum repeater R_i is defined via the terms of "Resource consumption of a quantum repeater" section, as

$$\mathscr{C}(R_i) := \sum_{k=1}^{z} \alpha(R_i, \mathrm{L}_l(k)). \tag{17}$$

Then, let $\chi(R_i)$ be the total number of received entangled states (number of Bell states) in R_i per cycle:

$$\chi(R_i) = \sum_{k=1}^{z} B_F(\mathrm{L}_l(k)), \tag{18}$$

which can be rewritten as a multiplication of the $|B_F(A)|$ number of entangled states outputted by a source node A to path $\mathscr{P}_s$, and a $\omega(\mathscr{P}_s) \in [0,1]$ weight of an s-th path $\mathscr{P}_s$, taken for all paths that pass through quantum repeater R_i between A and B, as

$$\chi(R_i) = \sum_{\forall \mathscr{P}_s(A,B) \in \mathscr{S}_{\mathscr{P}}(R_i)} \omega(\mathscr{P}_s(A,B)) \left| B_F(\mathscr{P}_s(A)) \right|, \tag{19}$$

where A and B are the source and target nodes associated with path $\mathscr{P}_s$; $\mathscr{S}_{\mathscr{P}}(R_i)$ is the set of $\mathscr{P}$ paths that pass through quantum repeater R_i between A and B, defined as

$$\mathscr{S}_{\mathscr{P}}(R_i) := \left\{ \mathscr{P}_s(x,y) \middle| R_i \in \mathscr{P}_s(x,y) \right\}, \tag{20}$$

with relation

$$\left| \mathscr{S}_{\mathscr{P}}(R_i, A, B) \right| \leq z; \tag{21}$$

where $\mathscr{P}_s(x,y)$ is a s-th path between quantum nodes x and y, $s = 1, \ldots, |\mathscr{S}_{xy}|$, where $\mathscr{S}_{xy}$ is the set of paths between x and y and $|\mathscr{S}_{xy}|$ is the cardinality of $\mathscr{S}_{xy}$; such that for a given source and target pair (A,B) of $\mathscr{P}_s$, $s = 1, \ldots, |\mathscr{S}_{AB}|$,

$$\sum_{s=1}^{|\mathscr{S}_{AB}|} \omega\left(\mathscr{P}_s(A,B)\right) = 1. \tag{22}$$

Using (18), the term in (17) can be rewritten as

$$\begin{aligned} \mathscr{C}\ (R_i) &\leq \chi(R_i) \sum_{k=1}^{z} \left(\partial(R_i, \mathrm{L}_l(k))\right) + \zeta(R_i, \mathrm{L}_l(k)) + C(R_i, \mathrm{L}_l(k)) \\ &= \sum_{\forall \mathscr{P}_s(A,B) \in \mathscr{S}_{\mathscr{P}}(R_i)} \sum_{k=1}^{z} \omega\left(\mathscr{P}_s(A,B)\right) |B_F\left(\mathscr{P}_s(A)\right)| \left(\partial(R_i, \mathrm{L}_l(k))\right) + \zeta(R_i, \mathrm{L}_l(k)) + C(R_i, \mathrm{L}_l(k)). \end{aligned} \tag{23}$$

The result in (23) reveals that a loose upper bound on $\mathscr{C}\ (R_i)$ can be obtained from (17) and (18), and also shows that $\mathscr{C}\ (R_i)$ is adjustable by the weight coefficients $\omega\left(\mathscr{P}_s\right)$. An aim here is therefore to find the optimal distribution of the weight coefficients.

Assuming that the total number of quantum repeaters is q, the optimization problem can be defined via an objective function $f\left(\mathscr{C}\ \right)$ subject to a minimization as

$$f\left(\mathscr{C}\ \right) := \min\left(\tilde{\mathscr{C}}\ (R_i)\right), \text{ for } 1 \leq i \leq q, \tag{24}$$

where

$$\tilde{\mathscr{C}}\ (R_i) = \max\left(\mathscr{C}\ (R_i)\right). \tag{25}$$

The problem is therefore to find the optimal distribution for the weights of the paths associated with the entangled connections that minimizes the objective function (24).

Using (22), a constraint $\Omega(R_i)$ can be defined for all source and target node pairs (x, y) that share an entangled connection $\mathrm{L}_l(x, y)$ through R_i, as

$$\Omega(R_i) := \sum_{s=1}^{|\mathscr{S}_{xy}|} \omega\left(\mathscr{P}_s(x,y)\right) = 1, \text{ for } \forall \mathrm{L}_l(x,y), \tag{26}$$

where

$$0 \leq \omega\left(\mathscr{P}_s(x,y)\right) \leq 1. \tag{27}$$

Then, let $B_F(R_i, R_j)$ be the entanglement throughput (Bell states per C) between quantum repeaters R_i and R_j connected by the entangled connection $\mathrm{L}_l(R_i, R_j)$, with an upper bound $B_F^*(R_i, R_j)$.

Using (19), a constraint $\Gamma\left(\mathrm{L}_l(R_i, R_j)\right)$ can be defined for the $\mathscr{P}$ paths that traverse an entangled connection $\mathrm{L}_l(R_i, R_j)$ between quantum repeaters R_i and R_j (see Fig. 2a), as

$$\Gamma\left(\mathrm{L}_l(R_i, R_j)\right) := \sum_{\forall \mathscr{P}_s(A,B) \in \mathscr{S}_{\mathscr{P}}^{\mathrm{L}_l(R_i,R_j)}(R_i) \bigcap \mathscr{S}_{\mathscr{P}}^{\mathrm{L}_l(R_i,R_j)}(R_j)} \omega\left(\mathscr{P}_s(A,B)\right) |B_F\left(\mathscr{P}_s(A)\right)| \leq B_F^*(R_i, R_j), \tag{28}$$

where $\mathscr{S}_{\mathscr{P}}^{\mathrm{L}_l(R_i,R_j)}(R_i) \bigcap \mathscr{S}_{\mathscr{P}}^{\mathrm{L}_l(R_i,R_j)}(R_j)$ refers to the set of paths that pass through the entangled connection $\mathrm{L}_l(R_i, R_j)$ between quantum repeaters R_i and R_j, respectively. As follows, in (28), a particular path

$$\mathscr{P}_s(A,B) = \mathrm{L}_l(A,B) \tag{29}$$

traverses the entangled connection $\mathrm{L}_l(R_i, R_j)$, if only the relation

$$\mathscr{P}_s(A,B) \in \mathscr{S}_{\mathscr{P}}^{\mathrm{L}_l(R_i,R_j)}(R_i) \bigcap \mathscr{S}_{\mathscr{P}}^{\mathrm{L}_l(R_i,R_j)}(R_j) \tag{30}$$

holds.

Then, let $\mathscr{S}_{\mathscr{P}}(N) = \{\mathscr{P}_1, \ldots, \mathscr{P}_n\}$ be the set of entangled paths, where $\mathscr{P}_i$ is an i-th entangled path, with a weighted entanglement throughput $\phi\left(\mathscr{P}_i\right)$ of the path $\mathscr{P}_i$ (Bell states per C), as

$$\phi\left(\mathscr{P}_i\right) = \omega\left(\mathscr{P}_i(A,B)\right) B_F\left(\mathscr{P}_i(A)\right), \tag{31}$$

where A is the source node of entangled path $\mathscr{P}_i$, $\omega\left(\mathscr{P}_i(A,B)\right)$ is the weight associated to $\mathscr{P}_i(A,B)$, while $B_F\left(\mathscr{P}_i(A)\right)$ is the entanglement throughput (Bell states per C) of the source node A of $\mathscr{P}_i$.

The optimal $D\left(\omega_s(x,y)\right)$ distribution of the weights that minimizes $f\left(\mathscr{C}\ \right)$ is determined via Procedure 1.

Procedure 1 assumes a quantum Internet scenario, in which a particular quantum repeater R_i has several different (logical) incoming and (logical) outcoming entangled connections, and the number of paths that traverse a particular quantum repeater is distributed non-uniformly. □

Procedure 1 Optimal distribution of entangled path weights

Input: A set $\mathscr{S}_{\mathscr{P}}(N)=\{\mathscr{P}_1,\ldots,\mathscr{P}_n\}$ of n entangled paths in N, where $\mathscr{P}_s(A,B)$ is an s-th path, $s=1,\ldots,n$, while A and B are the source and target quantum nodes of an s-th entangled path $\mathscr{P}_s$.
Output: Set $\mathscr{S}_D$ of optimal weights of the n entangled paths.

Step 1. Let N be a quantum network with a set of R_i, $i=1,\ldots,q$ quantum repeaters and a set $\mathscr{S}_{\mathscr{P}}(N)=\{\mathscr{P}_1,\ldots,\mathscr{P}_n\}$ of n entangled paths in N.
Step 2. For a given R_i, compute $\mathscr{C}(R_i)$ via (17). Determine $\chi(R_i)$ via (18), and for all paths that traverse R_i initialize the $\omega(\mathscr{P}_s(A,B))$ weights in (19), as

$$\omega(\mathscr{P}_s(A,B))=1,\ \text{for}\ \forall s.$$

Step 3. Repeat the steps for all the q quantum repeaters of N.
Step 4. Evaluate the $f(\mathscr{C})$ objective function via (24).
Step 5. Determine the $\xi(N)$ (Bell states per C) maximal and $\nu(N)$ (Bell states per C) minimal weighted entanglement throughputs of the paths in $\mathscr{S}_{\mathscr{P}}(N)$, as

$$\xi(N)=\max_{\forall s\in\mathscr{S}_{\mathscr{P}}(N)}\left(\omega(\mathscr{P}_s(A,B))B_F(\mathscr{P}_s(A))\right)$$

and

$$\nu(N)=\min_{\forall s\in\mathscr{S}_{\mathscr{P}}(N)}\left(\omega(\mathscr{P}_s(A,B))B_F(\mathscr{P}_s(A))\right)$$

and evaluate

$$\mu(N)=|\xi(N)-\nu(N)|.$$

Step 6. Set a target value $\mu^*(N)$ for $\mu(N)$.
If $\mu(N)<\mu^*(N)$, then redefine $\omega(\mathscr{P}_s(A,B))$ via a randomization operator $D(\cdot)$ as

$$D(\omega(\mathscr{P}_s(A,B)))$$

for $\forall\mathscr{P}_i$ paths of $\mathscr{S}_{\mathscr{P}}(N)$, until

$$\mu(N)\geq\mu^*(N)$$

is not satisfied, with constraints C_1 and C_2, as

$$C_1:=\left|\phi'(\mathscr{P}_i)-\phi(\mathscr{P}_i)\right|<\Delta(\phi(\mathscr{P}_i)),$$

where $\phi'(\mathscr{P}_i)$ is the updated weighted entanglement throughput of path $\mathscr{P}_i$ (Bell states per C), defined as

$$\phi'(\mathscr{P}_i):=D(\omega(\mathscr{P}_i(A,B)))B_F(\mathscr{P}_i(A)),$$

while $\Delta(\phi(\mathscr{P}_i))$ is an upper bound on the difference $|\phi'(\mathscr{P}_i)-\phi(\mathscr{P}_i)|$, and

$$C_2:=\frac{1}{n}\sum_{i=1}^{n}\phi'(\mathscr{P}_i)=\frac{1}{n}\sum_{i=1}^{n}\phi(\mathscr{P}_i).$$

If $\mu(N)\geq\mu^*(N)$, then goto Step 7.

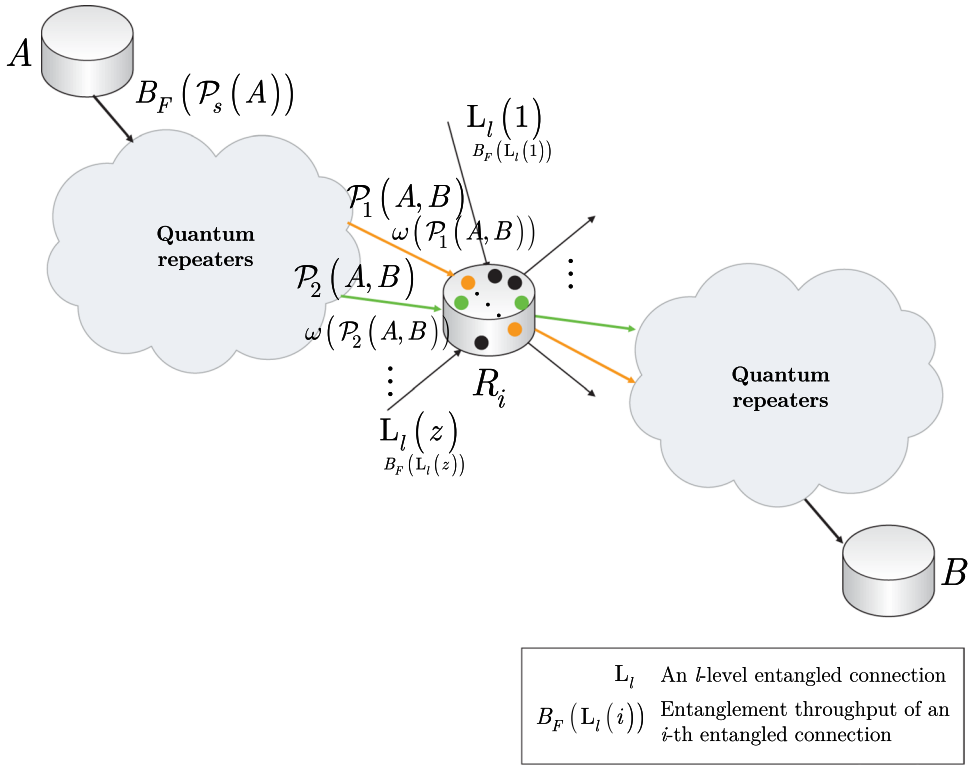

Figure 1. The schematic model of the resource consumption evaluation of a quantum repeater R_i in a quantum Internet scenario. The quantum repeater has z incoming entangled connections, $L_l(k)$, $k = 1, \ldots, z$, from among $|\mathscr{S}_{\mathscr{P}}(R_i)| = 2$ paths, $\mathscr{P}_s(A,B)$, $s = 1, 2$, that pass through quantum repeater R_i between A and B. The paths $\mathscr{P}_1(A,B)$ and $\mathscr{P}_2(A,B)$ are associated with the weighted entanglement throughput values $\omega(\mathscr{P}_1(A,B))B_F(\mathscr{P}_s(A))$ and $\omega(\mathscr{P}_2(A,B))B_F(\mathscr{P}_s(A))$, where $\omega(\mathscr{P}_s(A,B)) \in [0,1]$ are the path weights and $B_F(\mathscr{P}_s(A))$ is the entanglement throughput (Bell states per C) of the source A of the path $\mathscr{P}_s$. (The entangled states associated with the entangled connections in the quantum repeater are depicted by green, brown, and black dots.)

Procedure 1 Optimal distribution of entangled path weights (cont.)

Step 7. Using the updated $D(\omega(\mathscr{P}_s(A,B)))$ values, compute the updated $\mathscr{C}'(R_i)$ for all quantum repeaters, and re-evaluate the $f(\mathscr{C}')$ objective function (24).

Step 8. Set a $f^*(\mathscr{C})$ desired objective function value. Repeat steps 6-7, until

$$\begin{aligned}\Delta(f(\mathscr{C}')) &:= |f^*(\mathscr{C}) - f(\mathscr{C}')| \\ &= |\min(\tilde{\mathscr{C}}^*(R_i)) - \min(\tilde{\mathscr{C}}'(R_i))| \\ &= |\min(\max(\mathscr{C}^*(R_i))) - \min(\max(\mathscr{C}'(R_i)))|, \text{ for } 1 \le i \le q,\end{aligned}$$

does not reach a target value $\Delta^*(f(\mathscr{C}'))$, where $\min(\tilde{\mathscr{C}}^*(R_i))$ is a target value of the maximal resource consumption $\mathscr{C}^*(R_i)$ of quantum repeater R_i, while $\min(\tilde{\mathscr{C}}'(R_i))$ is the updated value.

Step 9. Output the set $\mathscr{S}_D$ of updated weights of the n entangled paths, as

$$\mathscr{S}_D = \{D(\omega(\mathscr{P}_1(A,B))), \ldots, D(\omega(\mathscr{P}_n(A,B)))\}.$$

The schematic model of the resource consumption determination of a quantum repeater is depicted in Fig. 1.

Entanglement swapping prioritization. Because the distribution of the weights $\omega(\mathscr{P}_s(A,B))$ is determined via Procedure 1, the task in a given quantum repeater is then to determine the set of entangled states associated with the weighted entangled connections for the entanglement swapping procedure.

Lemma 1 (Entanglement swapping probability and the weights of entangled connections). *The probability* $\Pr\left(U_S\left(\rho_A,\sigma_{B,i}\right)\right)$ *of entanglement swapping* U_S *between a source* ρ_A *and a target density matrix* $\sigma_{B,i}$ *in a quantum repeater depends on the weights associated with the swapped entangled connections.*

Proof Let

$$\Pr\left(U_S\left(\rho_A,\sigma_{B,i}\right)\right)=\Pr\left(\sigma_{B,i},R_s(\beta(\rho_A)),R_d\left(\beta\left(\sigma_{B,i}\right)\right)\right)$$

be the probability that density $\sigma_{B,i}$ is selected from $\mathscr{A}\left(\rho_A\right)$ to the entanglement swapping with ρ_A by swapping operator U_S.

Since set $\mathscr{A}\left(\rho_A\right)$ contains r possible entangled states for the entanglement swapping,

$$\sum_{i=1}^{r}\Pr\left(U_S\left(\rho_A,\sigma_{B,i}\right)\right)=\sum_{i=1}^{r}\Pr\left(\sigma_{B,i},R_s(\beta(\rho_A)),R_d\left(\beta\left(\sigma_{B,i}\right)\right)\right)=1, \tag{43}$$

where probability $\Pr\left(\sigma_{B,i},R_s(\beta(\rho_A)),R_d\left(\beta\left(\sigma_{B,i}\right)\right)\right)$ is evaluated as

$$\begin{aligned}&\Pr\left(\sigma_{B,i},R_s(\beta(\rho_A)),R_d\left(\beta\left(\sigma_{B,i}\right)\right)\right)\\&=\sum_{\forall\mathscr{P}_s(x,y)\in\kappa_{\mathscr{P}}}\omega_s\left(\mathrm{L}_l\left(R_s(\beta(\rho_A)),R_d\left(\beta\left(\sigma_{B,i}\right)\right)\right)\right)B_F\left(\mathrm{L}_l\left(R_s(\beta(\rho_A)),R_d\left(\beta\left(\sigma_{B,i}\right)\right)\right)\right),\end{aligned} \tag{44}$$

where

$$\kappa_{\mathscr{P}}=\mathscr{S}_{\mathscr{P}}\left(\sigma_{B,i},R_s(\beta(\rho_A)),R_d\left(\beta\left(\sigma_{B,i}\right)\right)\right), \tag{45}$$

and $B_F\left(\mathrm{L}_l\left(R_s(\beta(\rho_A)),R_d\left(\beta\left(\sigma_{B,i}\right)\right)\right)\right)$ is the entanglement throughput (Bell states per C) of the entangled connection $\mathrm{L}_l\left(R_s(\beta(\rho_A)),R_d\left(\beta\left(\sigma_{B,i}\right)\right)\right)$, while $\omega_s\left(\mathrm{L}_l\left(R_s(\beta(\rho_A)),R_d\left(\beta\left(\sigma_{B,i}\right)\right)\right)\right)$ is the weight associated with an s-th path over $\mathrm{L}_l\left(R_s(\beta(\rho_A)),R_d\left(\beta\left(\sigma_{B,i}\right)\right)\right)$ (see also Fig. 2a).

Assuming that for each $\sigma_{B,i}$ there exist a source set $\mathscr{Q}\left(\sigma_{B,i}\right)$ of g input entangled states,

$$\mathscr{Q}\left(\sigma_{B,i}\right)=\left\{\rho_{A,1},\ldots,\rho_{A,g}\right\}, \tag{46}$$

the probability $\Pr\left(\sigma_{B,i},\mathscr{Q}\left(\sigma_{B,i}\right),R_d\left(\beta\left(\sigma_{B,i}\right)\right)\right)$ can be yielded as

$$\begin{aligned}&\Pr\left(\sigma_{B,i},\mathscr{Q}\left(\sigma_{B,i}\right),R_d(\beta(\sigma_B))\right)\\&=\sum_{\forall\rho_{A,k}\in\mathscr{Q}\left(\sigma_{B,i}\right)}\sum_{\forall\mathscr{P}_s(x,y)\in\kappa_{\mathscr{P},k}}\omega_s\left(\mathrm{L}_l\left(R_s\left(\beta\left(\rho_{A,k}\right)\right),R_d\left(\beta\left(\sigma_{B,i}\right)\right)\right)\right)B_F\left(\mathrm{L}_l\left(R_s\left(\beta\left(\rho_{A,k}\right)\right),R_d\left(\beta\left(\sigma_{B,i}\right)\right)\right)\right),\end{aligned} \tag{47}$$

where

$$\kappa_{\mathscr{P},k}=\mathscr{S}_{\mathscr{P}}\left(\sigma_{B,i},R_s\left(\beta\left(\rho_{A,k}\right)\right),R_d\left(\beta\left(\sigma_{B,i}\right)\right)\right), \tag{48}$$

and

$$\sum_{i=1}^{r}\Pr\left(\sigma_{B,i},\mathscr{Q}\left(\sigma_{B,i}\right),R_d\left(\beta\left(\sigma_{B,i}\right)\right)\right)=1. \tag{49}$$

□

Entanglement swapping deadlock. The entangled state selection procedure of the entanglement swapping in a quantum repeater R_i can lead to a deadlock in the establishment of an entangled connection $L_l(R_i,R_d)$ between R_i, and a distant quantum repeater R_d.

An entanglement swapping situation in a quantum Internet scenario is depicted in Fig. 2b, c, respectively.

The problem of deadlock-free entanglement swapping is discussed in Section A.1 of the Supplemental Information.

Strongly-entangled structure for resource balancing in the quantum internet

A quantum network structure called the strongly-entangled quantum network is defined. The aim of this network is optimal resource balancing within the quantum Internet to take care of problematic situations. The problematic situation considered here is the serving of an arbitrary number of low-priority quantum nodes. A low-priority quantum node cannot be served by an actual quantum node in the network due to resource issues or an arbitrary network issue. Instead, the set of low-priority nodes are served through the strongly-entangled quantum network, which comprises an arbitrary number of quantum repeaters such that all quantum repeaters are entangled with each other. The strongly-entangled structure represents a resource that can manage issues in the network. In the serving procedure of the low-priority nodes, the quantum repeaters are selected uniformly at random to handle the density matrix of a low-priority node. The randomized behavior leads to a random routing between

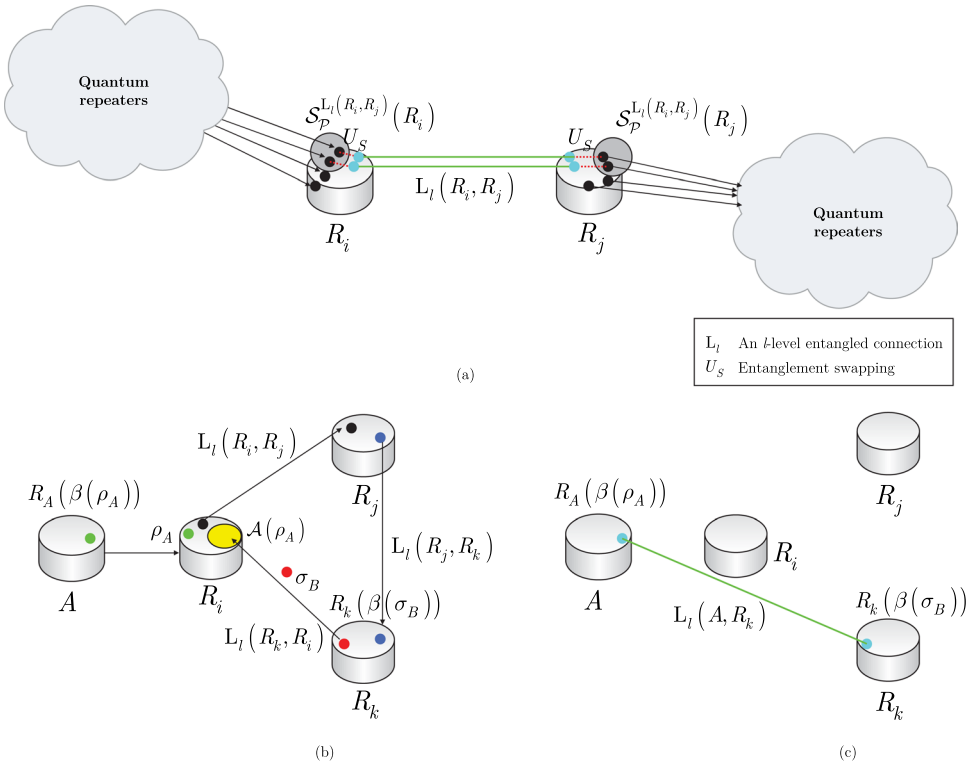

Figure 2. (**a**) A quantum Internet scenario with a set of incoming entangled connections $\mathcal{S}_{\mathcal{P}}^{\mathrm{L}_l(R_i,R_j)}(R_i) \bigcap \mathcal{S}_{\mathcal{P}}^{\mathrm{L}_l(R_i,R_j)}(R_j)$ that traverse the entangled connection $\mathrm{L}_l(R_i,R_j)$ between quantum repeaters R_i and R_j. The entangled states in the set $\mathcal{S}_{\mathcal{P}}^{\mathrm{L}_l(R_i,R_j)}(R_i)$ of R_i and in the set $\mathcal{S}_{\mathcal{P}}^{\mathrm{L}_l(R_i,R_j)}(R_j)$ of R_j (depicted by gray circles) are to be swapped with the entangled state that forms $\mathrm{L}_l(R_i,R_j)$. The entanglement swapping is performed by the entanglement swapping operator U_S. The other incoming entangled states in the quantum repeaters that do not traverse $\mathrm{L}_l(R_i,R_j)$ are not elements of $\mathcal{S}_{\mathcal{P}}^{\mathrm{L}_l(R_i,R_j)}(R_i) \bigcap \mathcal{S}_{\mathcal{P}}^{\mathrm{L}_l(R_i,R_j)}(R_j)$. (**b**) A deadlock situation in the entanglement swapping procedure in a quantum Internet setting. The aim of quantum node A is to share an entangled connection with the distant quantum repeater R_k. The source node A generates an entangled pair and transmits one half, ρ_A, to R_i and keeps the other half, $R_A(\beta(\rho_A))$. In R_i, the set $\mathcal{A}(\rho_A)$ (depicted by a yellow circle) does not contain the target entangled system σ_B from the target node R_k for the swapping; therefore, R_i generates an entangled pair (depicted by black dots) and shares an entangled connection $\mathrm{L}_l(R_i,R_j)$ with R_j. Quantum repeater R_j also generates an entangled pair (depicted by blue dots) and shares the entangled connection $\mathrm{L}_l(R_j,R_k)$ with R_k. Then, the target quantum node R_k generates an entangled connection (depicted by red dots) and sends one half, σ_B, to R_i to form the entangled connection $\mathrm{L}_l(R_k,R_i)$, while it keeps the other half, $R_k(\beta(\sigma_B))$. (c) Quantum repeater R_i receives σ_B and swaps it with ρ_A to form the distant entangled connection $\mathrm{L}_l(A,R_k)$. The deadlock in the entanglement swapping is caused by the fact that set $\mathcal{A}(\rho_A)$ in R_i does not contain σ_B, so R_i does not establish the entangled connection $\mathrm{L}_l(R_i,R_j)$ with R_j, and R_j does not establish the entangled connection $\mathrm{L}_l(R_j,R_k)$ with R_k.

the low-priority nodes and the quantum repeaters, as well as to optimal resource balancing within the network. It is also assumed that the strongly-entangled structure has connections with many subnetworks.

Resource allocation. In this section, the network situation is modeled via the definitions of "Strongly-entangled structure" section. A density matrix of R_i is associated with an $R_I^{\left(\mathcal{S}_{\mathcal{N}}\right)}$ ingress quantum repeater of $\mathcal{S}_{\mathcal{N}}$ selected uniformly at random, thus a random routing is performed for the incoming query from the low-priority node R_i to $\mathcal{S}_{\mathcal{N}}$. Then, an arbitrary routing is preformed between the $R_E^{\left(\mathcal{S}_{\mathcal{N}}\right)}$ egress quantum repeater of $\mathcal{S}_{\mathcal{N}}$ and the $D(R_i)$ destination node of R_i.

The quantum nodes and the entangled connections of the $\mathcal{S}_{\mathcal{N}}$ structure are characterized as follows. Let $R_q^{\left(\mathcal{S}_{\mathcal{N}}\right)}$ be an q-th, $q = 1, \ldots, \left|\mathcal{S}_{\mathcal{N}}\right|$, quantum repeater in $\mathcal{S}_{\mathcal{N}}$, and let $B\left(R_i^{\left(\mathcal{S}_{\mathcal{N}}\right)}, R_i\right)$ be the entanglement throughput request (Bell states per C) of the low-priority node R_i. The structure of a $\mathcal{S}_{\mathcal{N}}$ strongly-entangled quantum network is depicted in Fig. 4.

Theorem 2 (Handling resource issues via a strongly-entangled structure). *Let R_i be a low-priority quantum node with a non-servable resource request. The problem of resource allocation can be handled by a strongly-entangled quantum network structure $\mathscr{S}_{\mathscr{N}}$ and a random routing $\mathscr{R}$ between the quantum repeaters of $\mathscr{S}_{\mathscr{N}}$ and R_i.*

Proof The structure of $\mathscr{S}_{\mathscr{N}}$ allows to $R_q^{\left(\mathscr{S}_{\mathscr{N}}\right)}$ to split the $B\left(R_i^{\left(\mathscr{S}_{\mathscr{N}}\right)}, R_i\right)$ entanglement throughput request to $\left|\mathscr{S}_{\mathscr{N}}\right|$ smaller, $B\left(R_i^{\left(\mathscr{S}_{\mathscr{N}}\right)}, R_i\right) \Big/ \left|\mathscr{S}_{\mathscr{N}}\right|$ requests. As follows, within the structure of $\mathscr{S}_{\mathscr{N}}$, the entangled connection between quantum repeaters $R_i^{\left(\mathscr{S}_{\mathscr{N}}\right)}$ and $R_q^{\left(\mathscr{S}_{\mathscr{N}}\right)}$, is associated with the following entanglement throughput (Bell states per C):

$$Q\left(R_i^{\left(\mathscr{S}_{\mathscr{N}}\right)}, R_q^{\left(\mathscr{S}_{\mathscr{N}}\right)}\right) = \frac{B\left(R_i^{\left(\mathscr{S}_{\mathscr{N}}\right)}, R_i\right)}{\left|\mathscr{S}_{\mathscr{N}}\right|}, \text{ for } q = 1, \ldots, \left|\mathscr{S}_{\mathscr{N}}\right| - 1, q \neq i. \tag{50}$$

As follows, using $\mathscr{S}_{\mathscr{N}}$, the entanglement throughputs of all of the $\left|\mathscr{S}_{\mathscr{N}}\right| - 1$ entangled connections of $R_i^{\left(\mathscr{S}_{\mathscr{N}}\right)}$ are associated with the $1/\left|\mathscr{S}_{\mathscr{N}}\right|$-th of the incoming request of $R_i^{\left(\mathscr{S}_{\mathscr{N}}\right)}$. Therefore, the incoming of $R_i^{\left(\mathscr{S}_{\mathscr{N}}\right)}$ request is divided into $\left|\mathscr{S}_{\mathscr{N}}\right|$ fractions and distributed to the $\left|\mathscr{S}_{\mathscr{N}}\right| - 1$ neighbors of $R_i^{\left(\mathscr{S}_{\mathscr{N}}\right)}$ in the strongly-entangled structure $\mathscr{S}_{\mathscr{N}}$.

As the quantum repeaters of $\mathscr{S}_{\mathscr{N}}$ shared the entangled systems with each other, a random routing is utilized from all quantum repeaters of $\mathscr{S}_{\mathscr{N}}$ to the low-priority node R_i. The request from R_i to the strongly-entangled structure $\mathscr{S}_{\mathscr{N}}$ is served via

$$n_{\mathscr{P}} = \left|\mathscr{S}_{\mathscr{N}}\right| \tag{51}$$

parallel entangled paths $\mathscr{P}\left(R_q^{\left(\mathscr{S}_{\mathscr{N}}\right)}, R_i\right)$ between the quantum repeaters of $\mathscr{S}_{\mathscr{N}}$ and R_i.

Therefore, the source of a $\mathscr{P}\left(R_q^{\left(\mathscr{S}_{\mathscr{N}}\right)}, R_i\right)$ entangled path is the q-th quantum repeater $R_q^{\left(\mathscr{S}_{\mathscr{N}}\right)}$ from $\mathscr{S}_{\mathscr{N}}$, $q = 1, \ldots, \left|\mathscr{S}_{\mathscr{N}}\right|$, while the target is R_i. The $\left|\mathscr{S}_{\mathscr{N}}\right|$ parallel entangled paths define the set $\mathscr{R}_{\mathscr{S}}$ of random quantum repeaters used in the routing procedure as

$$\mathscr{R}_{\mathscr{S}} = \mathscr{R}\left(R_1^{\left(\mathscr{S}_{\mathscr{N}}\right)}, R_i\right) \bigcup \ldots \bigcup \mathscr{R}\left(R_{\left|\mathscr{S}_{\mathscr{N}}\right|}^{\left(\mathscr{S}_{\mathscr{N}}\right)}, R_i\right), \tag{52}$$

where $\mathscr{R}\left(R_i^{\left(\mathscr{S}_{\mathscr{N}}\right)}, R_i\right)$ identifies a set of random nodes used in the random routing $\mathscr{R}$ from $R_i^{\left(\mathscr{S}_{\mathscr{N}}\right)}$ to R_i.

As the entangled paths are established, an $U_S\left(R_q^{\left(\mathscr{S}_{\mathscr{N}}\right)}\right)$ entanglement swapping operation is applied in all of the $R_q^{\left(\mathscr{S}_{\mathscr{N}}\right)}$ quantum repeaters of $\mathscr{S}_{\mathscr{N}}$. The aim of these operations is to swap the entangled connections to the egress quantum repeater $R_E^{\left(\mathscr{S}_{\mathscr{N}}\right)}$ of $\mathscr{S}_{\mathscr{N}}$.

The result is $\left|\mathscr{S}_{\mathscr{N}}\right|$ entangled connections between R_i and $R_E^{\left(\mathscr{S}_{\mathscr{N}}\right)}$, i.e., the set of $\left|\mathscr{S}_{\mathscr{N}}\right|$ entangled paths

$$\mathscr{P}\ (R_i, B) = \mathscr{P}_1\left(R_i, R_E^{\left(\mathscr{S}_{\mathscr{N}}\right)}\right) \bigcup \ldots \bigcup \mathscr{P}_{\left|\mathscr{S}_{\mathscr{N}}\right|}\left(R_i, R_E^{\left(\mathscr{S}_{\mathscr{N}}\right)}\right) \tag{53}$$

such that the $B_F\left(\mathscr{P}\left(R_i, R_E^{\left(\mathscr{S}_{\mathscr{N}}\right)}\right)\right)$ entanglement throughput of entangled path $\mathscr{P}_j\left(R_i, R_E^{\left(\mathscr{S}_{\mathscr{N}}\right)}\right)$ is as

$$B_F\left(\mathscr{P}_j\left(R_i, R_E^{\left(\mathscr{S}_{\mathscr{N}}\right)}\right)\right) = B\left(R_q^{\left(\mathscr{S}_{\mathscr{N}}\right)}, R_i\right) = \frac{1}{\left|\mathscr{S}_{\mathscr{N}}\right|} B(R_i), \tag{54}$$

where $B(R_i)$ is the total entanglement throughput request of R_i (Bell states per C), since the entangled path of $R_q^{\left(\mathscr{S}_{\mathscr{N}}\right)}$ and R_i is swapped to the path between $R_E^{\left(\mathscr{S}_{\mathscr{N}}\right)}$ and R_i via a swapping $U_S\left(R_q^{\left(\mathscr{S}_{\mathscr{N}}\right)}\right)$ in $R_q^{\left(\mathscr{S}_{\mathscr{N}}\right)}$.

Therefore the sum of the entanglement throughput of the $\left|\mathscr{S}_{\mathscr{N}}\right|$ entangled paths (Bell states per C) is

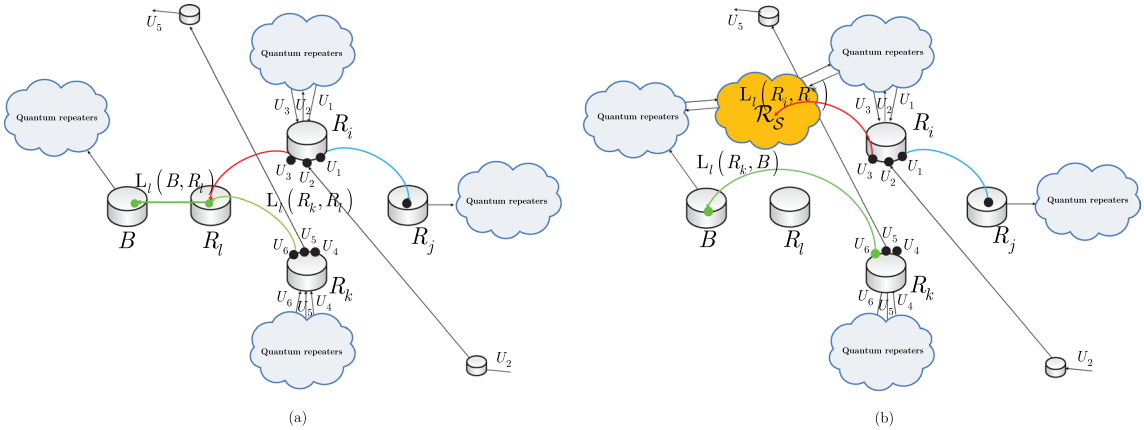

Figure 3. Entanglement distribution with resource balancing in the quantum Internet. (**a**) Low-priority quantum repeaters. Users U_3 and U_6 would like to share an entangled connection with B through R_l. Quantum repeater R_l has only a single density matrix from B available for the entanglement swapping via entangled connection $\mathrm{L_l(R_k, B)}$, and as a corollary, R_l can serve only U_3 or U_6. Users U_1, U_2, and U_5 are served directly, since these users have no common resource requirements. The quantum repeater node R_l serves U_6, thus establishing the entangled connection $\mathrm{L}_l(R_k, R_l)$ between R_k and R_l. (**b**) Resource balancing via random routing. User U_6 establishes the distant entangled connection $\mathrm{L}_l(R_k, B)$ with B through R_l (depicted by the green line). For a seamless transition of resource saving, a random quantum repeater is selected for user U_3 from the set $\mathscr{R}_{\mathscr{S}}$ of random quantum repeaters ($\mathscr{R}_{\mathscr{S}}$ is realized by the strongly-entangled structure $\mathscr{S}_{\mathscr{N}}$) to establish the entangled connection $\mathrm{L}_l(R_i, R^*)$ (depicted by the red line), where $R^* \in \mathscr{R}_{\mathscr{S}}$ is a quantum repeater from $\mathscr{R}_{\mathscr{S}}$.

$$\sum_{j=1}^{\left|\mathscr{S}_{\mathscr{N}}\right|} B_F\left(\mathscr{P}_j\left(R_i, R_E^{\left(\mathscr{S}_{\mathscr{N}}\right)}\right)\right) = \sum_{q=1}^{\left|\mathscr{S}_{\mathscr{N}}\right|} B\left(R_q^{\left(\mathscr{S}_{\mathscr{N}}\right)}, R_i\right) = B(R_i), \tag{55}$$

thus it equals to the entanglement throughput request received from the low-priority node R_i.

Assuming that there are n_c low-priority quantum nodes in N all with different entanglement throughput requests, the $\mathscr{S}_{\mathscr{N}}$ strongly-entangled structure has to serve all of these n_c low-priority quantum nodes simultaneously. In this case, the steps detailed above are established in parallel for all of the n_c low-priority nodes, thus the $n_{\Sigma\mathscr{P}}$ total number of parallel entangled connections established via the $\mathscr{S}_{\mathscr{N}}$ structure is

$$n_{\Sigma\mathscr{P}} = n_c\left|\mathscr{S}_{\mathscr{N}}\right|. \tag{56}$$

As the $\mathrm{L}_l\left(R_i, R_E^{\left(\mathscr{S}_{\mathscr{N}}\right)}\right)$ entangled connection is built up via the entanglement swapping in $R_I^{\left(\mathscr{S}_{\mathscr{N}}\right)}$, an arbitrary routing from $R_E^{\left(\mathscr{S}_{\mathscr{N}}\right)}$ to $D(R_i)$ can be used to construct the entangled connection $\mathrm{L}_l\left(R_E^{\left(\mathscr{S}_{\mathscr{N}}\right)}, D(R_i)\right)$. Then, an entanglement swapping in $R_E^{\left(\mathscr{S}_{\mathscr{N}}\right)}$ yields the long-distance $\mathrm{L}_l(R_i, D(R_i))$ entangled connection.

□

The construction method of a strongly-entangled structure is given Procedure 2.

Figure 3 depicts a quantum Internet scenario with the requirement of resource balancing in the quantum repeaters of the entanglement distribution process.

Procedure 2 Formulating and serving via the strongly-entangled structure

Input: Set $\mathscr{S}_{\mathscr{N}}$ of quantum repeaters with $|E(\mathscr{S}_{\mathscr{N}})| = \frac{|\mathscr{S}_{\mathscr{N}}|\cdot(|\mathscr{S}_{\mathscr{N}}|-1)}{2}$ entangled connections.
Output: Strongly entangled network structure within $\mathscr{S}_{\mathscr{N}}$.

Step 1. Set the $|\mathscr{S}_{\mathscr{N}}|$ number of quantum repeaters of $\mathscr{S}_{\mathscr{N}}$. Establish the $|E(\mathscr{S}_{\mathscr{N}})| = \frac{|\mathscr{S}_{\mathscr{N}}|\cdot(|\mathscr{S}_{\mathscr{N}}|-1)}{2}$ entangled connections of $\mathscr{S}_{\mathscr{N}}$.
Step 2. For a single density matrix ρ of a low-priority quantum repeater R_i, select uniformly at random an $R_I^{(\mathscr{S}_{\mathscr{N}})}$ ingress quantum repeater from $\mathscr{S}_{\mathscr{N}}$ with probability $\Pr\left(R_i \to R_I^{(\mathscr{S}_{\mathscr{N}})}\right) = \frac{1}{|\mathscr{S}_{\mathscr{N}}|}$ (or alternatively, the $R_I^{(\mathscr{S}_{\mathscr{N}})}$ quantum repeater starts to share an entangled system with R_i), to formulate the entangled connection $\mathrm{L}_l\left(R_i, R_I^{(\mathscr{S}_{\mathscr{N}})}\right)$ in $R_I^{(\mathscr{S}_{\mathscr{N}})}$. Apply a $U_S\left(R_I^{(\mathscr{S}_{\mathscr{N}})}\right)$ entanglement swapping in $R_I^{(\mathscr{S}_{\mathscr{N}})}$ to construct $\mathrm{L}_l\left(R_i, R_E^{(\mathscr{S}_{\mathscr{N}})}\right)$, with the $R_E^{(\mathscr{S}_{\mathscr{N}})}$ egress quantum repeater of $\mathscr{S}_{\mathscr{N}}$. Apply an arbitrary routing from $R_E^{(\mathscr{S}_{\mathscr{N}})}$ to $D(R_i)$ to establish $\mathrm{L}_l\left(R_E^{(\mathscr{S}_{\mathscr{N}})}, D(R_i)\right)$, and apply an entanglement swapping $U_S\left(R_E^{(\mathscr{S}_{\mathscr{N}})}\right)$ in $R_E^{(\mathscr{S}_{\mathscr{N}})}$ to construct the entangled connection $\mathrm{L}_l(R_i, D(R_i))$.
Step 3. At n_c low-priority R_i quantum repeaters, $i = 1, \ldots, n_c$, evaluate $\sum_{i=1}^{n_c} B(R_i)$, where $B(R_i)$ is the entanglement throughput request of $B(R_i)$. For all quantum repeaters of $\mathscr{S}_{\mathscr{N}}$, set the $B\left(R_q^{(\mathscr{S}_{\mathscr{N}})}, R_i\right)$ entanglement throughput request from R_i to $R_q^{(\mathscr{S}_{\mathscr{N}})}$ as $B\left(R_q^{(\mathscr{S}_{\mathscr{N}})}, R_i\right) = \frac{1}{|\mathscr{S}_{\mathscr{N}}|}B(R_i)$, $q = 1, \ldots, |\mathscr{S}_{\mathscr{N}}|$.
Step 4. Set the entanglement throughputs of the internal entangled connections of $\mathscr{S}_{\mathscr{N}}$, such that $Q\left(R_q^{(\mathscr{S}_{\mathscr{N}})}, R_z^{(\mathscr{S}_{\mathscr{N}})}\right) = \frac{1}{|\mathscr{S}_{\mathscr{N}}|}B\left(R_q^{(\mathscr{S}_{\mathscr{N}})}, R_i\right) = \frac{1}{|\mathscr{S}_{\mathscr{N}}|^2}B(R_i)$, where $R_z^{(\mathscr{S}_{\mathscr{N}})}$ is a neighbor of $R_q^{(\mathscr{S}_{\mathscr{N}})}$, $z \neq q$, $q = 1, \ldots, |\mathscr{S}_{\mathscr{N}}|$.
Step 5. Apply entanglement swapping from the $R_I^{(\mathscr{S}_{\mathscr{N}})}(R_i)$ ingress node of R_i to the $R_E^{(\mathscr{S}_{\mathscr{N}})}(R_i)$ egress node of R_i. For a given R_i, apply a $U_S\left(R_I^{(\mathscr{S}_{\mathscr{N}})}(R_i)\right)$ entanglement swapping in the ingress node $R_I^{(\mathscr{S}_{\mathscr{N}})}(R_i)$ of R_i to construct the entangled connection $\mathrm{L}_l\left(R_i, R_E^{(\mathscr{S}_{\mathscr{N}})}(R_i)\right)$.
Step 6. Apply an arbitrary routing between the $R_E^{(\mathscr{S}_{\mathscr{N}})}(R_i)$ egress quantum repeater and the $D(R_i)$ destination of the low-priority quantum repeater R_i.
Step 7. Apply an $U_S\left(R_E^{(\mathscr{S}_{\mathscr{N}})}(R_i)\right)$ entanglement swapping in the $R_E^{(\mathscr{S}_{\mathscr{N}})}(R_i)$ egress node associated with the served quantum repeater to construct the entangled connection $\mathrm{L}_l(R_i, D(R_i))$.
Step 8. Repeat steps 5-7 for all the n_c low-priority R_i quantum repeaters.

Resource balancing. **Theorem 3** (Capability of the strongly-entangled structure). *The strongly-entangled structure $\mathscr{S}_{\mathscr{N}}$ provides a structure to serve all the n_c low-priority quantum nodes simultaneously.*
Proof Using the metrics defined in "Capability of a strongly-entangled structure" section, first we derive some relevant attributes of $\mathscr{S}_{\mathscr{N}}$.

From (14), the $\mathscr{F}\left(R_q^{(\mathscr{S}_{\mathscr{N}})}\right)$ fanout (ratio of the $W\left(R_q^{(\mathscr{S}_{\mathscr{N}})}\right)$ total entanglement throughput (14) within $\mathscr{S}_{\mathscr{N}}$ and the $B\left(R_q^{(\mathscr{S}_{\mathscr{N}})}, \mathscr{S}_{n_c}\right)$ incoming request from the low-priority quantum repeaters, (12) of a quantum repeater $R_q^{(\mathscr{S}_{\mathscr{N}})}$ at n_c low-priority quantum repeaters is defined as

$$\begin{aligned}\mathscr{F}\left(R_q^{(\mathscr{S}_{\mathscr{N}})}\right) &:= \frac{W\left(R_q^{(\mathscr{S}_{\mathscr{N}})}\right)}{B\left(R_q^{(\mathscr{S}_{\mathscr{N}})}, \mathscr{S}_{n_c}\right)} \\ &= \frac{\left(|\mathscr{S}_{\mathscr{N}}|-1\right)\frac{1}{|\mathscr{S}_{\mathscr{N}}|^2}\left(\sum_{i=1}^{n_c} B(R_i)\right)}{\frac{1}{|\mathscr{S}_{\mathscr{N}}|}\left(\sum_{i=1}^{n_c} B(R_i)\right)} \\ &= \frac{1}{|\mathscr{S}_{\mathscr{N}}|}\left(|\mathscr{S}_{\mathscr{N}}|-1\right) \\ &= \left(1 - \frac{1}{|\mathscr{S}_{\mathscr{N}}|}\right),\end{aligned} \tag{57}$$

and the $\mathscr{F}(\mathscr{S}_{\mathscr{N}})$ fanout of $\mathscr{S}_{\mathscr{N}}$ as the maximum fanout among the quantum repeaters of $\mathscr{S}_{\mathscr{N}}$ as

$$\mathscr{F}\left(\mathscr{S}_{\mathscr{N}}\right) := \max_{q} \mathscr{F}\left(R_q^{\left(\mathscr{S}_{\mathscr{N}}\right)}\right) = \left(1 - \frac{1}{\left|\mathscr{S}_{\mathscr{N}}\right|}\right), \tag{58}$$

such that

$$\max_{q} \frac{W\left(R_q^{\left(\mathscr{S}_{\mathscr{N}}\right)}\right)}{\frac{1}{\left|\mathscr{S}_{\mathscr{N}}\right|^2}\left(\sum_{i=1}^{n_c} B(R_i)\right)} \geq \frac{Z\left(\mathscr{S}_{\mathscr{N}}\right)}{B\left(\mathscr{S}_{\mathscr{N}}\right)}, \tag{59}$$

by theory[135,136], where $Z\left(\mathscr{S}_{\mathscr{N}}\right)$ is as given in (15), while $B\left(\mathscr{S}_{\mathscr{N}}\right)$ is the total requests from the n_c quantum repeaters to $\mathscr{S}_{\mathscr{N}}$ (Bell states per C) as

$$B\left(\mathscr{S}_{\mathscr{N}}\right) = \sum_{q=1}^{\left|\mathscr{S}_{\mathscr{N}}\right|} B\left(R_q^{\left(\mathscr{S}_{\mathscr{N}}\right)}, \mathscr{S}_{n_c}\right) = \sum_{i=1}^{n_c} B(R_i). \tag{60}$$

Thus, (59) can be rewritten as

$$\mathscr{F}\left(\mathscr{S}_{\mathscr{N}}\right) = \frac{\left(\left|\mathscr{S}_{\mathscr{N}}\right|-1\right)\frac{1}{\left|\mathscr{S}_{\mathscr{N}}\right|}\left(\sum_{i=1}^{n_c} B(R_i)\right)}{\left|\mathscr{S}_{\mathscr{N}}\right|\left(\frac{1}{\left|\mathscr{S}_{\mathscr{N}}\right|}\left(\sum_{i=1}^{n_c} B(R_i)\right)\right)} = \left(1 - \frac{1}{\left|\mathscr{S}_{\mathscr{N}}\right|}\right). \tag{61}$$

As a corollary, $\mathscr{F}\left(\mathscr{S}_{\mathscr{N}}\right) \leq 1$ for any $\left|\mathscr{S}_{\mathscr{N}}\right| \geq 1$, while in a classical full-mesh structure $\mathscr{M}$, the fanout is lower bounded by 1, i.e. $\mathscr{F}\left(\mathscr{M}\right) \geq 1$. As follows, the $\mathscr{F}\left(\mathscr{S}_{\mathscr{N}}\right) \leq 1$ property is strictly resulted from the attributes of the quantum structure (such as entanglement swapping), and it cannot be achieved within any classical full-mesh structure-based uniform load-balancing[135,136].

Note, that in (61) it is assumed that within the structure of $\mathscr{S}_{\mathscr{N}}$, all the $R_q^{\left(\mathscr{S}_{\mathscr{N}}\right)}$ are associated with the same $B\left(R_q^{\left(\mathscr{S}_{\mathscr{N}}\right)}, \mathscr{S}_{n_c}\right)$ values (see (12)), and a corollary, the throughputs of the entangled connections within $\mathscr{S}_{\mathscr{N}}$ are set equally to $Q\left(R_q^{\left(\mathscr{S}_{\mathscr{N}}\right)}, R_z^{\left(\mathscr{S}_{\mathscr{N}}\right)}\right)$ (see (13)), since each quantum repeater receive the same amount of incoming request. Let us to derive $\mathscr{F}\left(\mathscr{S}_{\mathscr{N}}\right)$ for the case if the $B\left(R_q^{\left(\mathscr{S}_{\mathscr{N}}\right)}, \mathscr{S}_{n_c}\right)$ values of $\mathscr{S}_{\mathscr{N}}$ are not equally set, while the condition

$$\sum_{q=1}^{\left|\mathscr{S}_{\mathscr{N}}\right|} B\left(R_q^{\left(\mathscr{S}_{\mathscr{N}}\right)}, \mathscr{S}_{n_c}\right) = \sum_{i=1}^{n_c} B(R_i). \tag{62}$$

holds for the $B\left(R_q^{\left(\mathscr{S}_{\mathscr{N}}\right)}, \mathscr{S}_{n_c}\right)$ values in ingress quantum repeaters.

In this case, (15) is as

$$Z\left(\mathscr{S}_{\mathscr{N}}\right) = \sum_{q=1}^{\left|\mathscr{S}_{\mathscr{N}}\right|} \left(\left|\mathscr{S}_{\mathscr{N}}\right| - 1\right)\frac{1}{\left|\mathscr{S}_{\mathscr{N}}\right|} B\left(R_q^{\left(\mathscr{S}_{\mathscr{N}}\right)}, \mathscr{S}_{n_c}\right), \tag{63}$$

thus $\mathscr{F}\left(\mathscr{S}_{\mathscr{N}}\right)$ is yielded as

$$\begin{aligned} \mathscr{F}\left(\mathscr{S}_{\mathscr{N}}\right) &= \frac{\sum_{q=1}^{\left|\mathscr{S}_{\mathscr{N}}\right|}\left(\left|\mathscr{S}_{\mathscr{N}}\right|-1\right)\frac{1}{\left|\mathscr{S}_{\mathscr{N}}\right|} B\left(R_q^{\left(\mathscr{S}_{\mathscr{N}}\right)}, \mathscr{S}_{n_c}\right)}{B\left(\mathscr{S}_{\mathscr{N}}\right)} \\ &= \frac{\left(\left(\left|\mathscr{S}_{\mathscr{N}}\right|-1\right)\frac{1}{\left|\mathscr{S}_{\mathscr{N}}\right|}\right)\sum_{i=1}^{n_c} B(R_i)}{\sum_{i=1}^{n_c} B(R_i)} \\ &= \left(\left|\mathscr{S}_{\mathscr{N}}\right| - 1\right)\frac{1}{\left|\mathscr{S}_{\mathscr{N}}\right|}, \end{aligned} \tag{64}$$

thus (64) picks up its minimum (61) if the incoming density matrices of $\mathscr{S}_{\mathscr{N}}$ are not uniformly distributed.

On the other hand, if

$$\sum_{q=1}^{\left|\mathscr{S}_{\mathscr{N}}\right|} B\left(R_q^{\left(\mathscr{S}_{\mathscr{N}}\right)}, \mathscr{S}_{n_c}\right) < \sum_{i=1}^{n_c} B(R_i), \tag{65}$$

such that

$$\sum_{q=1}^{\left|\mathscr{S}_{\mathscr{N}}\right|} B\left(R_q^{\left(\mathscr{S}_{\mathscr{N}}\right)}, \mathscr{S}_{n_c}\right) + x = \sum_{i=1}^{n_c} B(R_i) \tag{66}$$

while the internal entangled connections of $\mathscr{S}_{\mathscr{N}}$ are set with relation $\sum_q Q\left(R_q^{\left(\mathscr{S}_{\mathscr{N}}\right)}, R_z^{\left(\mathscr{S}_{\mathscr{N}}\right)}\right) = \sum_{i=1}^{n_c} B(R_i)$, then

$$\begin{aligned} \mathscr{F}\left(\mathscr{S}_{\mathscr{N}}\right) &= \frac{\left(\left(\left|\mathscr{S}_{\mathscr{N}}\right|-1\right)\frac{1}{\left|\mathscr{S}_{\mathscr{N}}\right|}\right)\sum_{i=1}^{n_c} B(R_i)}{B\left(\mathscr{S}_{\mathscr{N}}\right)-x} \\ &> \left(\left|\mathscr{S}_{\mathscr{N}}\right|-1\right)^{\frac{1}{\left|\mathscr{S}_{\mathscr{N}}\right|}}. \end{aligned} \tag{67}$$

On the relation of the incoming request and the internal entanglement throughputs of the entangled connections some derivations are as follows.

Let $B\left(R_q^{\left(\mathscr{S}_{\mathscr{N}}\right)}, \mathscr{S}_{n_c}\right)$ be the entanglement throughput request from the n_c low-priority nodes to $R_q^{\left(\mathscr{S}_{\mathscr{N}}\right)}$ (Bell states per C), and let $R_E^{\left(\mathscr{S}_{\mathscr{N}}\right)}$ be the egress node of the requests with entangled connection $\mathrm{L}_l\left(R_q^{\left(\mathscr{S}_{\mathscr{N}}\right)}, R_E^{\left(\mathscr{S}_{\mathscr{N}}\right)}\right)$.

If the entanglement throughput $Q\left(R_q^{\left(\mathscr{S}_{\mathscr{N}}\right)}, R_E^{\left(\mathscr{S}_{\mathscr{N}}\right)}\right)$ within $\mathscr{S}_{\mathscr{N}}$ is set as

$$Q\left(R_q^{\left(\mathscr{S}_{\mathscr{N}}\right)}, R_E^{\left(\mathscr{S}_{\mathscr{N}}\right)}\right) \geq B\left(R_q^{\left(\mathscr{S}_{\mathscr{N}}\right)}, \mathscr{S}_{n_c}\right), \tag{68}$$

then a request from $R_q^{\left(\mathscr{S}_{\mathscr{N}}\right)}$ to $R_E^{\left(\mathscr{S}_{\mathscr{N}}\right)}$ can be served, while if

$$Q\left(R_q^{\left(\mathscr{S}_{\mathscr{N}}\right)}, R_E^{\left(\mathscr{S}_{\mathscr{N}}\right)}\right) < B\left(R_q^{\left(\mathscr{S}_{\mathscr{N}}\right)}, \mathscr{S}_{n_c}\right), \tag{69}$$

the request $B\left(R_q^{\left(\mathscr{S}_{\mathscr{N}}\right)}, \mathscr{S}_{n_c}\right)$ is served through different $\mathrm{L}_l\left(R_i^{\left(\mathscr{S}_{\mathscr{N}}\right)}, R_j^{\left(\mathscr{S}_{\mathscr{N}}\right)}\right)$ entangled connections in $\mathscr{S}_{\mathscr{N}}$, such that

$$\sum_{i<j} Q\left(R_i^{\left(\mathscr{S}_{\mathscr{N}}\right)}, R_j^{\left(\mathscr{S}_{\mathscr{N}}\right)}\right) \geq Q\left(R_q^{\left(\mathscr{S}_{\mathscr{N}}\right)}, R_E^{\left(\mathscr{S}_{\mathscr{N}}\right)}\right), \tag{70}$$

and

$$\sum_{i<j} Q\left(R_i^{\left(\mathscr{S}_{\mathscr{N}}\right)}, R_j^{\left(\mathscr{S}_{\mathscr{N}}\right)}\right) \geq B\left(R_q^{\left(\mathscr{S}_{\mathscr{N}}\right)}, \mathscr{S}_{n_c}\right). \tag{71}$$

Assuming that (68) holds for all quantum repeaters of $\mathscr{S}_{\mathscr{N}}$, then

$$\sum_{q\neq E} Q\left(R_q^{\left(\mathscr{S}_{\mathscr{N}}\right)}, R_E^{\left(\mathscr{S}_{\mathscr{N}}\right)}\right) \geq \sum_{q\neq E} B\left(R_q^{\left(\mathscr{S}_{\mathscr{N}}\right)}, \mathscr{S}_{n_c}\right), \tag{72}$$

while if $q = E$, then the $R_q^{\left(\mathscr{S}_{\mathscr{N}}\right)}$ node is also the egress node, thus the aim is to achieve an arbitrary routing from $R_q^{\left(\mathscr{S}_{\mathscr{N}}\right)}$ to the distant node associated with the incoming request that is not part of the structure $\mathscr{S}_{\mathscr{N}}$.

The proof is concluded here. □

The schematic model of the strongly-entangled structure $\mathscr{S}_{\mathscr{N}}$ is illustrated in Fig. 4.

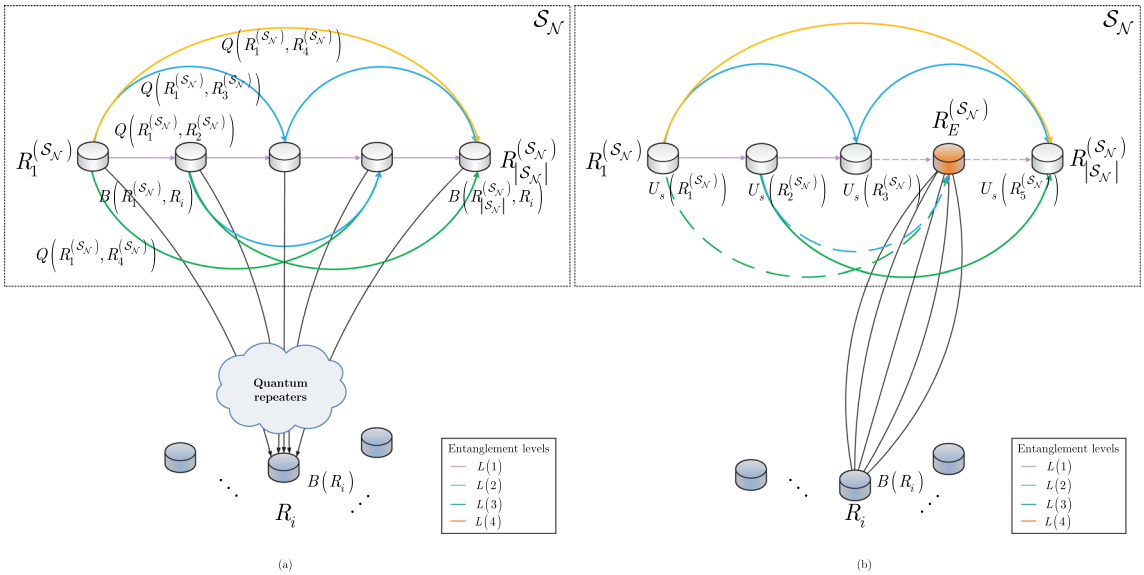

Figure 4. The strongly-entangled structure $\mathscr{S}_{\mathscr{N}}$ as formed by $|\mathscr{S}_{\mathscr{N}}|$ quantum repeaters and $|E(\mathscr{S}_{\mathscr{N}})|$ entangled connections with heterogeneous entanglement levels, where $|\mathscr{S}_{\mathscr{N}}| = 5, |E(\mathscr{S}_{\mathscr{N}})| = \frac{|\mathscr{S}_{\mathscr{N}}| \cdot (|\mathscr{S}_{\mathscr{N}}| - 1)}{2}$, and $\mathscr{F}(\mathscr{S}_{\mathscr{N}}) = \left(1 - \frac{1}{|\mathscr{S}_{\mathscr{N}}|}\right)$. (**a**) The low-priority node R_i is associated with the entanglement throughput request $B(R_i)$. The $|\mathscr{S}_{\mathscr{N}}|$ quantum repeaters of $\mathscr{S}_{\mathscr{N}}$ establish $|\mathscr{S}_{\mathscr{N}}|$ entangled connections with R_i (depicted by the outgoing dashed black lines), with each connection having entanglement throughput $B\left(R_q^{(\mathscr{S}_{\mathscr{N}})}, R_i\right) = \frac{1}{|\mathscr{S}_{\mathscr{N}}|} B(R_i)$, where $\sum_{q=1}^{|\mathscr{S}_{\mathscr{N}}|} B\left(R_q^{(\mathscr{S}_{\mathscr{N}})}, R_i\right) = B(R_i)$. A given quantum repeater $R_q^{(\mathscr{S}_{\mathscr{N}})}$ of $\mathscr{S}_{\mathscr{N}}$ establishes $|\mathscr{S}_{\mathscr{N}}| - 1$ entangled connections within $\mathscr{S}_{\mathscr{N}}$, each with entanglement throughput $Q\left(R_q^{(\mathscr{S}_{\mathscr{N}})}, R_z^{(\mathscr{S}_{\mathscr{N}})}\right) = \frac{1}{|\mathscr{S}_{\mathscr{N}}|} B\left(R_q^{(\mathscr{S}_{\mathscr{N}})}, R_i\right)$, where $R_z^{(\mathscr{S}_{\mathscr{N}})}$ is a neighbor of $R_q^{(\mathscr{S}_{\mathscr{N}})}$. (**b**) Each of the $|\mathscr{S}_{\mathscr{N}}| - 1$ quantum repeaters of $\mathscr{S}_{\mathscr{N}}$ applies entanglement swapping U_S to establish the entangled connection between R_i and the egress quantum repeater $R_E^{(\mathscr{S}_{\mathscr{N}})}$ of $\mathscr{S}_{\mathscr{N}}$. Then, an arbitrary routing is applied to establish the entangled connection between R_i and the destination node $D(R_i)$ of R_i. The request from R_i to the strongly-entangled structure $\mathscr{S}_{\mathscr{N}}$ is served via $n_{\mathscr{P}} = |\mathscr{S}_{\mathscr{N}}|$ parallel entangled paths $\mathscr{P}\left(R_q^{(\mathscr{S}_{\mathscr{N}})}, R_i\right)$ between the quantum repeaters of $\mathscr{S}_{\mathscr{N}}$ and R_i. The dashed entangled connections are rebuilt within $\mathscr{S}_{\mathscr{N}}$ after the entanglement swapping operations.

Lemma 2 (Resource-balancing efficiency of the strongly-entangled structure $\mathscr{S}_{\mathscr{N}}$ for n_c low-priority nodes).*In terms of fanout minimization and total traffic minimization, the strongly-entangled quantum network structure $\mathscr{S}_{\mathscr{N}}$ is two times more efficient than a classical full-mesh network structure $\mathscr{M}$.*

Proof First, we compare the fanout coefficients of the classical full-mesh structure $\mathscr{M}$ and the strongly-entangled quantum network $\mathscr{S}_{\mathscr{N}}$. Then, we compare the total amount of traffic within the structures of $\mathscr{M}$ and $\mathscr{S}_{\mathscr{N}}$.

For simplicity, let us assume that $|\mathscr{M}| = |\mathscr{S}_{\mathscr{N}}|$ and that the nodes of the structures are associated with the same incoming traffic (measured in the number of packets for $\mathscr{M}$, and the number of density matrices for $\mathscr{S}_{\mathscr{N}}$):

$$T\left(x_q^{(\mathscr{M})}, x_i\right) = B\left(R_q^{(\mathscr{S}_{\mathscr{N}})}, R_i\right), \tag{73}$$

where $T(\cdot)$ is the traffic of $\mathscr{M}$, $B(\cdot)$ is the traffic of $\mathscr{S}_{\mathscr{N}}$, x_i is a source node, $x_q^{(\mathscr{M})}$ is the q-th node of $\mathscr{M}$, R_i is a source quantum repeater, and $R_q^{(\mathscr{S}_{\mathscr{N}})}$ is the q-th quantum repeater of $\mathscr{S}_{\mathscr{N}}$.

It can be verified[135,136], that for structure $\mathscr{M}$, the fanout coefficient $\mathscr{F}(\mathscr{M})$ is

$$\mathscr{F}(\mathscr{M}) = 2(|\mathscr{M}| - 1)\frac{1}{|\mathscr{M}|} = 2\left(1 - \frac{1}{|\mathscr{M}|}\right), \tag{74}$$

where $\mathcal{F}\left(\mathcal{S}_{\mathcal{N}}\right)$ is as in (58). The fanout of the entangled structure is half of the fanout of $\mathcal{M}$; thus, $\mu\left(\mathcal{F}\left(\mathcal{S}_{\mathcal{N}}\right), \mathcal{F}\left(\mathcal{M}\right)\right)$, the ratio of $\mathcal{F}\left(\mathcal{S}_{\mathcal{N}}\right)$ to $\mathcal{F}\left(\mathcal{M}\right)$, trivially follows: $\mu\left(\mathcal{F}\left(\mathcal{S}_{\mathcal{N}}\right), \mathcal{F}\left(\mathcal{M}\right)\right) = \frac{\mathcal{F}\left(\mathcal{S}_{\mathcal{N}}\right)}{\mathcal{F}\left(\mathcal{M}\right)} = \frac{1}{2}$.

Therefore, in terms of fanout minimization, the strongly-entangled structure is two times more efficient than a classical full-mesh structure.

In terms of the total traffic required within the structures, the results are as follows.

It can be proven that in the classical full-mesh structure $\mathcal{M}$, two phases of communications are required to establish a communication between a low-priority node x_i and an egress node $x_E^{(\mathcal{M})}$ of $\mathcal{M}$. In the first phase, the ingress node $x_I^{(\mathcal{M})}$ of $\mathcal{M}$ transmits the incoming packet to a random intermediate node of $\mathcal{M}$. In the second phase, the packet is transmitted from $x_z^{(\mathcal{M})}$ to the exit node $x_E^{(\mathcal{M})}$ of $\mathcal{M}$. Accordingly, an incoming packet traverses $\mathcal{M}$ twice[135,136].

On the other hand, in the strongly-entangled structure $\mathcal{S}_{\mathcal{N}}$, only the first phase is required for seamless routing. The second step can be replaced via the entanglement swapping operator; thus, the incoming densities can be entangled with the target node without a second phase transmission.

In $\mathcal{S}_{\mathcal{N}}$, all quantum repeaters share an entangled connection with the low-priority node; thus, in a quantum repeater $R_q^{\left(\mathcal{S}_{\mathcal{N}}\right)}$ of $\mathcal{S}_{\mathcal{N}}$ only an entanglement swapping $U_S\left(R_q^{\left(\mathcal{S}_{\mathcal{N}}\right)}\right)$ is required to establish an entangled connection between the low-priority node R_i and the egress quantum repeater $R_E^{\left(\mathcal{S}_{\mathcal{N}}\right)}$ of $\mathcal{S}_{\mathcal{N}}$. Therefore, as the entangled path is established from $R_E^{\left(\mathcal{S}_{\mathcal{N}}\right)}$ to $D(R_i)$, a swapping $U_S\left(R_E^{\left(\mathcal{S}_{\mathcal{N}}\right)}\right)$ in $R_E^{\left(\mathcal{S}_{\mathcal{N}}\right)}$ connects $D(R_i)$ with the low-priority node R_i. Accordingly, in the strongly-entangled structure $\mathcal{S}_{\mathcal{N}}$, it is enough to apply only one phase to serve R_i via $R_E^{\left(\mathcal{S}_{\mathcal{N}}\right)}$, whereas $\mathcal{M}$ requires two phases.

The corollaries for the amount of traffic within the structures are as follows. In $\mathcal{M}$, each node uniformly load-balances its incoming traffic to the other nodes of the structure, regardless of the destination, and then all packets are delivered to the final destination via an egress node by an arbitrary routing[135,136]. The two phases within $\mathcal{M}$ require a total traffic

$$T\left(x_i, \mathcal{M}\right) = \frac{2\left(|\mathcal{M}|-1\right)T\left(x_I^{(\mathcal{M})}, x_i\right)}{|\mathcal{M}|}. \tag{75}$$

In $\mathcal{S}_{\mathcal{N}}$, since only the first phase is required, it reduces the total traffic to

$$B\left(R_i, \mathcal{S}_{\mathcal{N}}\right) = \frac{\left(\left|\mathcal{S}_{\mathcal{N}}\right|-1\right)B\left(R_q^{\left(\mathcal{S}_{\mathcal{N}}\right)}, R_i\right)}{\left|\mathcal{S}_{\mathcal{N}}\right|}; \tag{76}$$

thus from (75) and (76), the ratio of the total transmissions within $\mathcal{M}$ and $\mathcal{S}_{\mathcal{N}}$ is

$$\mu(R_i, x_i) = \frac{B\left(R_i, \mathcal{S}_{\mathcal{N}}\right)}{T\left(x_i, \mathcal{M}\right)} = \frac{1}{2}. \tag{77}$$

Then, let us further assume that there are n_c low-priority nodes with a node set $\mathcal{S}_{n_c}$ and that each node $x_i^{(\mathcal{M})}$ of $\mathcal{M}$ is an ingress node receiving incoming traffic $T\left(x_{I,i}^{(\mathcal{M})}, S_i^{n_c}\right)$ from $S_i^{n_c}$, where $S_i^{n_c}$ is the i-th subset of $\mathcal{S}_{n_c}$.

In this case, the total traffic in $\mathcal{M}$ is $T\left(\mathcal{S}_{n_c}, \mathcal{M}\right) = \sum_{i=1}^{|\mathcal{M}|} \frac{2\left(|\mathcal{M}|-1\right)T\left(x_{I,i}^{(\mathcal{M})}, S_i^{n_c}\right)}{|\mathcal{M}|}$, whereas for the structure $\mathcal{S}_{\mathcal{N}}$,

$$B\left(\mathcal{S}_{n_c}, \mathcal{S}_{\mathcal{N}}\right) = \sum_{q=1}^{\left|\mathcal{S}_{\mathcal{N}}\right|} \frac{\left(\left|\mathcal{S}_{\mathcal{N}}\right|-1\right)B\left(R_q^{\left(\mathcal{S}_{\mathcal{N}}\right)}, S_i^{n_c}\right)}{\left|\mathcal{S}_{\mathcal{N}}\right|}; \tag{78}$$

thus, the ratio of the total traffic in the structures is also $1/2$, since

$$\mu\left(\mathcal{S}_{\mathcal{N}}, \mathcal{M}\right) = \frac{B\left(\mathcal{S}_{n_c}, \mathcal{S}_{\mathcal{N}}\right)}{T\left(\mathcal{S}_{n_c}, \mathcal{M}\right)} = \frac{1}{2}. \tag{79}$$

Assuming that the incoming traffic is the same for all ingress nodes in the structures of $\mathcal{M}$ and $\mathcal{S}_{\mathcal{N}}$, the result in (5.2) simplifies as

$$T\left(\mathcal{S}_{n_c}, \mathcal{M}\right) = \frac{|\mathcal{M}|\left(|\mathcal{M}|-1\right)}{2}\frac{2T\left(x_I^{(\mathcal{M})}, S_i^{n_c}\right)}{|\mathcal{M}|} = \left(|\mathcal{M}|-1\right)T\left(x_I^{(\mathcal{M})}, S_i^{n_c}\right), \tag{80}$$

while (78) can be rewritten as

$$B\left(\mathscr{S}_{n_c},\mathscr{S}_{\mathscr{N}}\right)=\frac{\left|\mathscr{S}_{\mathscr{N}}\right|\left(\left|\mathscr{S}_{\mathscr{N}}\right|-1\right)}{2}\frac{B\left(R_q^{\left(\mathscr{S}_{\mathscr{N}}\right)},S_i^{n_c}\right)}{\left|\mathscr{S}_{\mathscr{N}}\right|}=\frac{\left(\left|\mathscr{S}_{\mathscr{N}}\right|-1\right)}{2}B\left(R_q^{\left(\mathscr{S}_{\mathscr{N}}\right)},S_i^{n_c}\right);\tag{81}$$

thus the ratio of (79) also follows.

As a corollary, using the total entanglement throughput $T\left(\mathscr{S}_{\mathscr{N}}\right)$ (16) of the entangled connections of $\mathscr{S}_{\mathscr{N}}$ (Bell states per C) and the total traffic $T\left(\mathscr{M}\right)$ of $\mathscr{M}$,

$$T\left(\mathscr{M}\right)=\left(\left|\mathscr{M}\right|-1\right)\left(\sum_{i=1}^{n_c}T(x_i)\right),\tag{82}$$

the ratio

$$\mu\left(T\left(\mathscr{S}_{\mathscr{N}}\right),T\left(\mathscr{M}\right)\right)=\frac{T\left(\mathscr{S}_{\mathscr{N}}\right)}{T\left(\mathscr{M}\right)}=\frac{1}{2}\tag{83}$$

follows.

Therefore, with respect to the amount of total traffic, the proposed strongly-entangled network structure $\mathscr{S}_{\mathscr{N}}$ is two times more efficient than a classical full-mesh network structure $\mathscr{M}$.

The proof is concluded here. □

Random routing. **Theorem 4** (Random routing efficiency via the strongly-entangled structure). *The structure $\mathscr{S}_{\mathscr{N}}$ enables an efficient random routing for all the n_c low-priority quantum repeaters $R_i, i=1,\ldots,n_c$, via the total number of entanglement swapping operations $\left|U_S\left(\mathscr{S}_{\mathscr{N}},R_i\right)\right|$ in $\mathscr{S}_{\mathscr{N}}$ for the serving of R_i, with* $\Pr\left(\left|U_S\left(\mathscr{S}_{\mathscr{N}},R_i\right)\right|\geq 2c\right)\leq\frac{1}{2^{\left|\mathscr{S}_{\mathscr{N}}\right|}}$, *for any $c\geq 1$.*

Proof Our aim here is to show that the probability that more than entanglement swapping operation is required in a particular uniform randomly selected $R_I^{\left(\mathscr{S}_{\mathscr{N}}\right)}$ ingress quantum repeater of $\mathscr{S}_{\mathscr{N}}$ to construct the entangled path between the source R_i and egress quantum repeater $R_E^{\left(\mathscr{S}_{\mathscr{N}}\right)}$ of $\mathscr{S}_{\mathscr{N}}$ is low.

Let $\left|\mathscr{S}_{\mathscr{N}}\right|$ be the number of $R_q^{\left(\mathscr{S}_{\mathscr{N}}\right)}$ quantum repeaters, $q=1,\ldots,\left|\mathscr{S}_{\mathscr{N}}\right|$ in the strongly-entangled structure $\mathscr{S}_{\mathscr{N}}$, and let $\left|E\left(\mathscr{S}_{\mathscr{N}}\right)\right|$ be the number of entangled connections within $\mathscr{S}_{\mathscr{N}}$, $\left|E\left(\mathscr{S}_{\mathscr{N}}\right)\right|=\frac{\left|\mathscr{S}_{\mathscr{N}}\right|\cdot\left(\left|\mathscr{S}_{\mathscr{N}}\right|-1\right)}{2}$.

Then, let R_i a source quantum node from the set $\mathscr{S}_{n_c}$ of the n_c low-priority quantum repeaters, $\left|\mathscr{S}_{n_c}\right|=n_c$. Then, a given $R_I^{\left(\mathscr{S}_{\mathscr{N}}\right)}$ ingress quantum repeater is selected for R_i with probability

$$\Pr\left(R_i\rightarrow R_I^{\left(\mathscr{S}_{\mathscr{N}}\right)}\right)=\frac{1}{\left|\mathscr{S}_{\mathscr{N}}\right|},\tag{84}$$

to formulate the random entangled path $\mathscr{P}_i$ from R_i to $R_I^{\left(\mathscr{S}_{\mathscr{N}}\right)}$,

$$\mathscr{P}_i=\mathscr{P}\left(R_I^{\left(\mathscr{S}_{\mathscr{N}}\right)},R_i\right).\tag{85}$$

Then, let assume that a random path $\mathscr{P}_i$ requires the egress quantum repeater $R_E^{\left(\mathscr{S}_{\mathscr{N}}\right)}$, that formulates entangled path between R_i and $R_I^{\left(\mathscr{S}_{\mathscr{N}}\right)}$

$$\mathscr{P}_i=\mathscr{P}\left(R_E^{\left(\mathscr{S}_{\mathscr{N}}\right)},R_i\right).\tag{86}$$

Let $f(\cdot)$ be an indicator function, defined as

$$f\left(\mathscr{P}_i,\mathscr{P}_j\right):=\begin{cases}1,\ \text{if}\left(R_I^{\left(\mathscr{S}_{\mathscr{N}}\right)}\left(\mathscr{P}_i\right)=R_I^{\left(\mathscr{S}_{\mathscr{N}}\right)}\left(\mathscr{P}_j\right)\right)\wedge\left(R_E^{\left(\mathscr{S}_{\mathscr{N}}\right)}\left(\mathscr{P}_i\right)=R_E^{\left(\mathscr{S}_{\mathscr{N}}\right)}\left(\mathscr{P}_j\right)\right),\\ 0,\ \text{otherwise}\end{cases}\tag{87}$$

where $R_I^{\left(\mathscr{S}_{\mathscr{N}}\right)}\left(\mathscr{P}_x\right)\in\mathscr{S}_{\mathscr{N}}$ and $R_E^{\left(\mathscr{S}_{\mathscr{N}}\right)}\left(\mathscr{P}_x\right)\in\mathscr{S}_{\mathscr{N}}$ are the ingress and egress quantum repeaters of path $\mathscr{P}_x$. Thus, the indicator function indicates an event if the $R_I^{\left(\mathscr{S}_{\mathscr{N}}\right)}\left(\mathscr{P}_i\right)$ ingress node of $\mathscr{P}_i$ coincidences with the

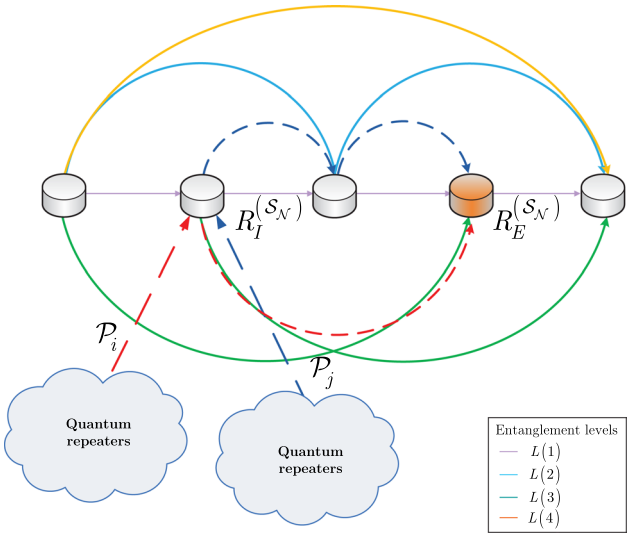

Figure 5. A collision of entangled paths in the strongly-entangled structure. The ingress and egress quantum repeaters associated with the paths within the strongly-entangled structure coincide. Entangled path $\mathscr{P}_i$ is depicted by a red dashed line, and entangled path $\mathscr{P}_j$ is depicted by a blue dashed line.

$R_I^{(\mathcal{S}_\mathcal{N})}(\mathscr{P}_j)$ ingress node of $\mathscr{P}_j$ and the $R_E^{(\mathcal{S}_\mathcal{N})}(\mathscr{P}_i)$ egress node of $\mathscr{P}_i$ coincidences with the $R_E^{(\mathcal{S}_\mathcal{N})}(\mathscr{P}_j)$ egress node of $\mathscr{P}_j$. Thus, a $f(\mathscr{P}_i, \mathscr{P}_j) = 1$ situation therefore indicates a collision between the paths $\mathscr{P}_i$ and $\mathscr{P}_j$ (A collision situation is illustrated in Fig. 5.).

Since for $\mathscr{P}_i$ and $\mathscr{P}_j$, the $R_I^{(\mathcal{S}_\mathcal{N})}$ ingress quantum repeaters are selected independently and uniformly random within $\mathcal{S}_{n_c}$, it follows that for the entangled paths $\{\mathscr{P}_i, \mathscr{P}_j, \mathscr{P}_k\}$, the $f(\mathscr{P}_i, \mathscr{P}_j)$ and $f(\mathscr{P}_i, \mathscr{P}_k)$ indicator functions are independent random variables for $i \neq j \neq k \neq i$.

As follows, indicator functions $f(\mathscr{P}_i, \mathscr{P}_j)$ and $f(\mathscr{P}_i, \mathscr{P}_k)$ can be rewritten as Bernoulli random variables

$$X_j = f(\mathscr{P}_i, \mathscr{P}_j) \tag{88}$$

and

$$X_k = f(\mathscr{P}_i, \mathscr{P}_k), \tag{89}$$

such that

$$\Pr(X_j = 1) = \mathbb{E}[X_j] \leq \frac{\left|\mathscr{P}_{\mathcal{S}_\mathcal{N}}\right|}{\left|E(\mathcal{S}_\mathcal{N})\right|}, \tag{90}$$

where $\left|\mathscr{P}_{\mathcal{S}_\mathcal{N}}\right|$ is the path length within $\mathcal{S}_\mathcal{N}$, such that

$$\left|\mathscr{P}_{\mathcal{S}_\mathcal{N}}\right| = 1 \tag{91}$$

due to the structural attributes of $\mathcal{S}_\mathcal{N}$. (Thus, (91) holds because only one entangled connection within $\mathcal{S}_\mathcal{N}$ is required for the swapping from the ingress node to an egress node.).

As follows, (90) can be rewritten as

$$\Pr(X_j = 1) = \mathbb{E}[X_j] \leq \frac{1}{\frac{\left|\mathcal{S}_\mathcal{N}\right| \cdot \left(\left|\mathcal{S}_\mathcal{N}\right| - 1\right)}{2}} = \frac{2}{\left|\mathcal{S}_\mathcal{N}\right| \cdot \left(\left|\mathcal{S}_\mathcal{N}\right| - 1\right)} \tag{92}$$

Taking (92) for all the $\left|\mathcal{S}_\mathcal{N}\right|$ nodes, yields a tail distribution for the sum of $\left|\mathcal{S}_\mathcal{N}\right|$ Bernoulli variables, as

$$\Pr(X_\Sigma \geq x), \tag{93}$$

where X_Σ is the sum of $\left|\mathcal{S}_\mathcal{N}\right|$ Bernoulli random variables,

$$X_\Sigma = \sum_{j=1}^{\left|\mathcal{S}_\mathcal{N}\right|} X_j, \tag{94}$$

for any positive x, with a relation by Markov inequality

$$\Pr\left(X_{\Sigma} \geq x\right) \leq \frac{\left|\mathscr{S}_{\mathscr{N}}\right|\mathbb{E}\left[X_j\right]}{x} = \frac{\left|\mathscr{S}_{\mathscr{N}}\right|\frac{2}{\left|\mathscr{S}_{\mathscr{N}}\right|\cdot\left(\left|\mathscr{S}_{\mathscr{N}}\right|-1\right)}}{x} = \frac{2}{x\left(\left|\mathscr{S}_{\mathscr{N}}\right|-1\right)} \leq \frac{1}{x}. \tag{95}$$

Then, since (95) is not sufficiently small if

$$x = 2c \tag{96}$$

for any constant c, (95) can be reformulated as

$$\Pr\left(X_{\Sigma} \geq x\right) \leq \Pr\left(e^{nX_{\Sigma}} \geq e^{nx}\right) \leq \frac{\mathbb{E}\left[e^{nX_{\Sigma}}\right]}{e^{nx}}, \tag{97}$$

for any positive n.

Thus, from the Chernoff-bound[181], the relation

$$\Pr\left(X_{\Sigma} \geq x\right) \leq \min_{n>0} \frac{\mathbb{E}\left[e^{nX_{\Sigma}}\right]}{e^{nx}}, \tag{98}$$

follows.

Since X_{Σ} is the sum of $\left|\mathscr{S}_{\mathscr{N}}\right|$ Bernoulli random variables, $\mathbb{E}\left[e^{nX_{\Sigma}}\right]$ can be evaluated as

$$\begin{aligned}
\mathbb{E}\left[e^{nX_{\Sigma}}\right] &= \mathbb{E}\left[e^{n\sum_{j=1}^{\left|\mathscr{S}_{\mathscr{N}}\right|} X_j}\right] \\
&= \prod_{j=1}^{\left|\mathscr{S}_{\mathscr{N}}\right|} \mathbb{E}\left[e^{nX_j}\right] \\
&= \left(\mathbb{E}\left[e^{nX_j}\right]\right)^{\left|\mathscr{S}_{\mathscr{N}}\right|} \\
&= \left(pe^{n} + \left(1-p\right)\right)^{\left|\mathscr{S}_{\mathscr{N}}\right|} \\
&= \left(1 + p\left(e^{n}-1\right)\right)^{\left|\mathscr{S}_{\mathscr{N}}\right|},
\end{aligned} \tag{99}$$

that can be rewritten as

$$\mathbb{E}\left[e^{nX_{\Sigma}}\right] \leq e^{\left(e^{n}-1\right)\left|\mathscr{S}_{\mathscr{N}}\right|\mathbb{E}\left[X_j\right]}, \tag{100}$$

since $1 + a \leq e^{a}$, by theory.

Therefore, $\Pr\left(X_{\Sigma} \geq x\right)$ can be rewritten as

$$\Pr\left(X_{\Sigma} \geq x\right) = \min_{n>0} \frac{e^{\left(e^{n}-1\right)\left|\mathscr{S}_{\mathscr{N}}\right|\mathbb{E}\left[X_j\right]}}{e^{nx}}, \tag{101}$$

thus at

$$n = \ln\left(1+\xi\right) \tag{102}$$

the following relation is yielded

$$\Pr\left(X_{\Sigma} \geq \left(1+\xi\right)\left|\mathscr{S}_{\mathscr{N}}\right|\mathbb{E}\left[X_j\right]\right) \leq \left(\frac{e^{\xi}}{\left(1+\xi\right)^{1+\xi}}\right)^{\left|\mathscr{S}_{\mathscr{N}}\right|\mathbb{E}\left[X_j\right]}. \tag{103}$$

It can be verified, that if ξ is sufficiently large, then (103) can be rewritten as

$$\Pr\left(X_{\Sigma} \geq c\left|\mathscr{S}_{\mathscr{N}}\right|\mathbb{E}\left[X_j\right]\right) \leq \left(\frac{1}{2}\right)^{\left|\mathscr{S}_{\mathscr{N}}\right|\mathbb{E}\left[X_j\right]}, \tag{104}$$

thus the probability that for a given resource node R_i with path $\mathscr{P}_i$ more than one $U_S\left(\mathscr{S}_{\mathscr{N}}, R_i\right)$ entanglement swapping operation is required within $\mathscr{S}_{\mathscr{N}}$ to construct the entangled path between R_i and $R_E^{\left(\mathscr{S}_{\mathscr{N}}\right)}\left(\mathscr{P}_i\right)$, is yielded as

$$\Pr\left(\left|U_S\left(\mathscr{S}_{\mathscr{N}}, R_i\right)\right| \geq 2c\right) \leq \frac{1}{2^{\left|\mathscr{S}_{\mathscr{N}}\right|}}, \tag{105}$$

where $c \geq 1$ is a positive integer, while $\left|U_S\left(\mathscr{S}_{\mathscr{N}}, R_i\right)\right|$ is the number of entanglement swapping operations within $\mathscr{S}_{\mathscr{N}}$ associated with R_i.

The proof is therefore concluded here. □

A path collision between entangled paths $\mathscr{P}_i$ and $\mathscr{P}_j$ in the strongly-entangled structure $\mathscr{S}_{\mathscr{N}}$ is illustrated in Fig. 5. Both entangled paths are associated with the same ingress node $R_I^{\left(\mathscr{S}_{\mathscr{N}}\right)}\left(\mathscr{P}_i\right) = R_I^{\left(\mathscr{S}_{\mathscr{N}}\right)}\left(\mathscr{P}_j\right)$ and egress node $R_E^{\left(\mathscr{S}_{\mathscr{N}}\right)}\left(\mathscr{P}_i\right) = R_E^{\left(\mathscr{S}_{\mathscr{N}}\right)}\left(\mathscr{P}_j\right)$. Assuming that $R_I^{\left(\mathscr{S}_{\mathscr{N}}\right)}$ and $R_E^{\left(\mathscr{S}_{\mathscr{N}}\right)}$ share only one entangled connection within $\mathscr{S}_{\mathscr{N}}$, only the serving of one path from $R_I^{\left(\mathscr{S}_{\mathscr{N}}\right)}$ to $R_E^{\left(\mathscr{S}_{\mathscr{N}}\right)}$ is allowed. Path $\mathscr{P}_i$ is served via the entangled connection between $R_I^{\left(\mathscr{S}_{\mathscr{N}}\right)}$ and $R_E^{\left(\mathscr{S}_{\mathscr{N}}\right)}$, while the serving of $\mathscr{P}_j$ is decomposed as $R_I^{\left(\mathscr{S}_{\mathscr{N}}\right)} \rightarrow R_z^{\left(\mathscr{S}_{\mathscr{N}}\right)} \rightarrow R_E^{\left(\mathscr{S}_{\mathscr{N}}\right)}$, where $R_z^{\left(\mathscr{S}_{\mathscr{N}}\right)} \neq R_E^{\left(\mathscr{S}_{\mathscr{N}}\right)}$.

Fault tolerance. **Theorem 5** (Fault tolerance of the strongly-entangled structure). *The strongly-entangled structure provides a seamless service at* $1 \leq k \leq \left|\mathscr{S}_{\mathscr{N}}\right| - 2$ *arbitrary entangled connection failures by increasing the entanglement throughputs of the remaining* $\left|E\left(\mathscr{S}_{\mathscr{N}}\right)\right| - k$ *entangled connections of* $\mathscr{S}_{\mathscr{N}}$.

Proof Let $Q\left(R_q^{\left(\mathscr{S}_{\mathscr{N}}\right)}, R_z^{\left(\mathscr{S}_{\mathscr{N}}\right)}\right) = \frac{1}{\left|\mathscr{S}_{\mathscr{N}}\right|} B\left(R_q^{\left(\mathscr{S}_{\mathscr{N}}\right)}, R_i\right)$ be the entanglement throughputs (see (50)) of the entangled connections within $\mathscr{S}_{\mathscr{N}}$ at no failures.

At k entangled connection failures, let Δ_k be the increment of the entanglement throughputs (Bell states per C) of the remaining $\left|E\left(\mathscr{S}_{\mathscr{N}}\right)\right| - k$ entangled connections of $\mathscr{S}_{\mathscr{N}}$, and let

$$Q_k^*\left(R_q^{\left(\mathscr{S}_{\mathscr{N}}\right)}, R_z^{\left(\mathscr{S}_{\mathscr{N}}\right)}\right) = Q\left(R_q^{\left(\mathscr{S}_{\mathscr{N}}\right)}, R_z^{\left(\mathscr{S}_{\mathscr{N}}\right)}\right) + \Delta_k \tag{106}$$

be the updated entanglement throughputs of the entangled connections of $\mathscr{S}_{\mathscr{N}}$ (Bell states per C).

Let us define entangled connection failure events E_1, E_2 and E_3 in the following manner:

$$\mathrm{E} := \begin{cases} \mathrm{E}_1, \text{ if } k = 1 \\ \mathrm{E}_2, \text{ if } (k = 2) \vee \left(k = \left|\mathscr{S}_{\mathscr{N}}\right| - 2\right) \vee \left(\left|\mathscr{S}_{\mathscr{N}}\right| \leq 6\right) \\ \mathrm{E}_3, \text{ otherwise.} \end{cases} \tag{107}$$

Then, using the formalisms of[136], after some calculations Δ_k can be evaluated as

$$\Delta_k = \begin{cases} \frac{1}{2}\left(\frac{1}{\left|\mathscr{S}_{\mathscr{N}}\right|-2} B\left(R_q^{\left(\mathscr{S}_{\mathscr{N}}\right)}, \mathscr{S}_{n_c}\right) + \frac{1}{\left|\mathscr{S}_{\mathscr{N}}\right|} B\left(R_q^{\left(\mathscr{S}_{\mathscr{N}}\right)}, \mathscr{S}_{n_c}\right)\right) - \frac{1}{\left|\mathscr{S}_{\mathscr{N}}\right|} B\left(R_q^{\left(\mathscr{S}_{\mathscr{N}}\right)}, \mathscr{S}_{n_c}\right), \text{ if } \mathrm{E} = \mathrm{E}_1 \\ \frac{1}{2}\left(\frac{1}{\left|\mathscr{S}_{\mathscr{N}}\right|-k-1} B\left(R_q^{\left(\mathscr{S}_{\mathscr{N}}\right)}, \mathscr{S}_{n_c}\right) + \frac{1}{\left|\mathscr{S}_{\mathscr{N}}\right|-1} B\left(R_q^{\left(\mathscr{S}_{\mathscr{N}}\right)}, \mathscr{S}_{n_c}\right)\right) - \frac{1}{\left|\mathscr{S}_{\mathscr{N}}\right|} B\left(R_q^{\left(\mathscr{S}_{\mathscr{N}}\right)}, \mathscr{S}_{n_c}\right), \text{ if } \mathrm{E} = \mathrm{E}_2 \\ \left(\frac{1}{\left|\mathscr{S}_{\mathscr{N}}\right|-k} B\left(R_q^{\left(\mathscr{S}_{\mathscr{N}}\right)}, \mathscr{S}_{n_c}\right)\right) - \frac{1}{\left|\mathscr{S}_{\mathscr{N}}\right|} B\left(R_q^{\left(\mathscr{S}_{\mathscr{N}}\right)}, \mathscr{S}_{n_c}\right), \text{ if } \mathrm{E} = \mathrm{E}_3. \end{cases} \tag{108}$$

As follows, at an initial $Q\left(R_q^{\left(\mathscr{S}_{\mathscr{N}}\right)}, R_z^{\left(\mathscr{S}_{\mathscr{N}}\right)}\right) = \frac{1}{\left|\mathscr{S}_{\mathscr{N}}\right|} B\left(R_q^{\left(\mathscr{S}_{\mathscr{N}}\right)}, R_i\right)$, the updated $Q_k^*\left(R_q^{\left(\mathscr{S}_{\mathscr{N}}\right)}, R_z^{\left(\mathscr{S}_{\mathscr{N}}\right)}\right)$ at the failure of k entangled connections in $\mathscr{S}_{\mathscr{N}}$ is on the order of

$$Q_k^*\left(R_q^{\left(\mathscr{S}_{\mathscr{N}}\right)}, R_z^{\left(\mathscr{S}_{\mathscr{N}}\right)}\right) \cong \frac{1}{\left|\mathscr{S}_{\mathscr{N}}\right|-k} B\left(R_q^{\left(\mathscr{S}_{\mathscr{N}}\right)}, \mathscr{S}_{n_c}\right). \tag{109}$$

As h quantum repeater $R_q^{\left(\mathscr{S}_{\mathscr{N}}\right)}$ fails within $\mathscr{S}_{\mathscr{N}}$, then the structure of $\mathscr{S}_{\mathscr{N}}$ becomes a strongly-entangled network formulated by $\left|\mathscr{S}_{\mathscr{N}}\right| - h$ quantum repeaters, therefore Δ_h is yielded as

$$\Delta_h = \frac{1}{\left|\mathscr{S}_{\mathscr{N}}\right|-k} B\left(R_q^{\left(\mathscr{S}_{\mathscr{N}}\right)}, \mathscr{S}_{n_c}\right) - \frac{1}{\left|\mathscr{S}_{\mathscr{N}}\right|} B\left(R_q^{\left(\mathscr{S}_{\mathscr{N}}\right)}, \mathscr{S}_{n_c}\right). \tag{110}$$

If both k entangled connections and h quantum repeater $R_q^{\left(\mathscr{S}_{\mathscr{N}}\right)}$ fails in the structure, then the problem is analogous to k entangled connection failures within a strongly-entangled structure formulated by $\left|\mathscr{S}_{\mathscr{N}}\right| - h$ quantum repeaters[135,136]. Therefore, $\Delta_{k,h}$ can be evaluated via (108) and (110) in the following manner:

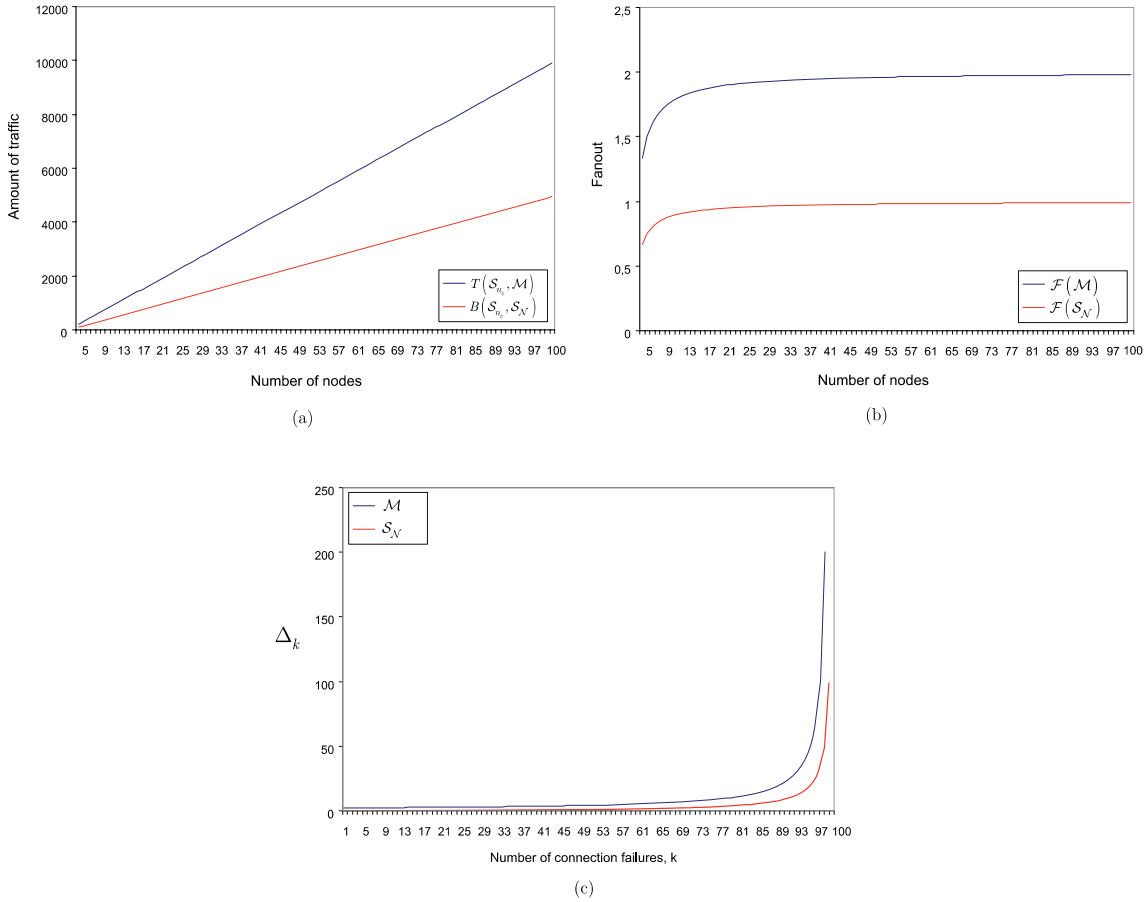

Figure 6. (**a**) Comparison of the amounts of traffic $T\left(\mathscr{S}_{n_c}, \mathscr{M}\right)$ and $B\left(\mathscr{S}_{n_c}, \mathscr{S}_{\mathscr{N}}\right)$ (Bell states per C) within the structures of $\mathscr{M}$ and $\mathscr{S}_{\mathscr{N}}$, with $T\left(x_I^{(\mathscr{M})}, S_i^{n_c}\right) = B\left(R_q^{\left(\mathscr{S}_{\mathscr{N}}\right)}, S_i^{n_c}\right) = 100$ and $\left|\mathscr{M}\right| = \left|\mathscr{S}_{\mathscr{N}}\right| = 1, \ldots, 100$. (**b**) Comparison of the fanout coefficients $\mathscr{F}\left(\mathscr{M}\right)$ and $\mathscr{F}\left(\mathscr{S}_{\mathscr{N}}\right)$ of the structures of $\mathscr{M}$ and $\mathscr{S}_{\mathscr{N}}$, with $\left|\mathscr{M}\right| = \left|\mathscr{S}_{\mathscr{N}}\right| = 1, \ldots, 100$. (**c**) The entanglement throughput increment Δ_k (Bell states per C) of the $\left|E\left(\mathscr{S}_{\mathscr{N}}\right)\right| - k$ entangled connections at the failure of k entangled connections within $\mathscr{S}_{\mathscr{N}}$, with $k = 1, \ldots, 100$, $\left|\mathscr{S}_{\mathscr{N}}\right| = 100$, $B\left(R_q^{\left(\mathscr{S}_{\mathscr{N}}\right)}, R_i\right) = 100$, and $Q\left(R_q^{\left(\mathscr{S}_{\mathscr{N}}\right)}, R_z^{\left(\mathscr{S}_{\mathscr{N}}\right)}\right) = \frac{1}{\left|\mathscr{S}_{\mathscr{N}}\right|} B\left(R_q^{\left(\mathscr{S}_{\mathscr{N}}\right)}, R_i\right) = 1$, $Q_k^*\left(R_q^{\left(\mathscr{S}_{\mathscr{N}}\right)}, R_z^{\left(\mathscr{S}_{\mathscr{N}}\right)}\right) \cong \frac{1}{\left|\mathscr{S}_{\mathscr{N}}\right| - k} B\left(R_q^{\left(\mathscr{S}_{\mathscr{N}}\right)}, \mathscr{S}_{n_c}\right)$. For the comparison between classical resource balancing and quantum resource balancing, the proposed results are compared with the results of[135,136].

$$\Delta_{k,h} = \begin{cases} \frac{1}{2}\left(\frac{1}{\left(\left|\mathscr{S}_{\mathscr{N}}\right|-h\right)-2} B\left(R_q^{\left(\mathscr{S}_{\mathscr{N}}\right)}, \mathscr{S}_{n_c}\right) + \frac{1}{\left|\mathscr{S}_{\mathscr{N}}\right|-h} B\left(R_q^{\left(\mathscr{S}_{\mathscr{N}}\right)}, \mathscr{S}_{n_c}\right)\right) - \frac{1}{\left|\mathscr{S}_{\mathscr{N}}\right|} B\left(R_q^{\left(\mathscr{S}_{\mathscr{N}}\right)}, \mathscr{S}_{n_c}\right), & \text{if } \mathrm{E} = \mathrm{E}_1 \\ \frac{1}{2}\left(\frac{1}{\left(\left|\mathscr{S}_{\mathscr{N}}\right|-h\right)-k-1} B\left(R_q^{\left(\mathscr{S}_{\mathscr{N}}\right)}, \mathscr{S}_{n_c}\right) + \frac{1}{\left(\left|\mathscr{S}_{\mathscr{N}}\right|-h\right)-1} B\left(R_q^{\left(\mathscr{S}_{\mathscr{N}}\right)}, \mathscr{S}_{n_c}\right)\right) - \frac{1}{\left|\mathscr{S}_{\mathscr{N}}\right|} B\left(R_q^{\left(\mathscr{S}_{\mathscr{N}}\right)}, \mathscr{S}_{n_c}\right), & \text{if } \mathrm{E} = \mathrm{E}_2 \\ \left(\frac{1}{\left(\left|\mathscr{S}_{\mathscr{N}}\right|-h\right)-k} B\left(R_q^{\left(\mathscr{S}_{\mathscr{N}}\right)}, \mathscr{S}_{n_c}\right)\right) - \frac{1}{\left|\mathscr{S}_{\mathscr{N}}\right|} B\left(R_q^{\left(\mathscr{S}_{\mathscr{N}}\right)}, \mathscr{S}_{n_c}\right), & \text{if } \mathrm{E} = \mathrm{E}_3. \end{cases} \tag{111}$$

□

Performance evaluation

Here, we analyze the performance of the strongly-entangled structure $\mathscr{S}_{\mathscr{N}}$ and compare it with a classical full-mesh structure $\mathscr{M}$. Using the results of "Method" and "Strongly-entangled structure for resource balancing in the quantum internet" sections, a numerical evidence is given to characterize the amount of transmitted traffic within the structures as a function of the number of nodes, to characterize the fanout coefficients of the structures

as a function of the number of nodes, and to compare the traffic increments of the connections at connection failures. For the comparison between classical resource balancing and quantum resource balancing, the results of "Method" and "Strongly-entangled structure for resource balancing in the quantum internet" sections are compared with the results of[135,136].

In Fig. 6a the amounts of traffic are compared within a strongly-entangled structure $\mathscr{S}_{\mathscr{N}}$ and a classical full-mesh structure $\mathscr{M}$. In Fig. 6b, the fanout coefficients of the structures are compared. In Fig. 6c compares the fault tolerant capabilities of the structures.

The strongly-entangled quantum network is two times more effective than a classical full-mesh structure: The required amount of traffic is half that of the classical structure[135,136], the fanout coefficient of the strongly-entangled structure is half that of the classical structure, and the required entanglement throughput of the entangled connection is half that of the classical structure. As future work, our aim is to provide a detailed performance comparison with other related approaches on resource allocation and routing in quantum networks[62,70,71].

Conclusions

Here, we defined methods and procedures for optimizing the resource allocation mechanisms of the quantum Internet. We proposed a model for resource consumption optimization of quantum repeaters, proposed a method for optimizing the entanglement swapping procedure, and studied the conditions of deadlock-free entanglement swapping. We defined a strongly-entangled network structure for optimal resource balancing in the quantum Internet. We proved the resource-balancing efficiency of the strongly-entangled structure and its fault tolerance.

Data availability

This work does not have any experimental data.

Received: 23 September 2020; Accepted: 2 December 2020
Published online: 28 December 2020

References

1. Gyongyosi, L. & Imre, S. *Resource Prioritization and Resource Balancing for the Quantum Internet, FIO19 Proceedings*. Washington DC. United States. https://doi.org/10.1364/FIO.2019.JTu4A.47 (2019).
2. Van Meter, R. *Quantum Networking*. ISBN 1118648927, 9781118648926, Wiley (2014).
3. Lloyd, S. *et al.* Infrastructure for the quantum internet. *ACM SIGCOMM Compu. Commun. Rev.* **34**, 9–20 (2004).
4. Kimble, H. J. The quantum internet. *Nature* **453**, 1023–1030 (2008).
5. Gyongyosi, L. *Services for the Quantum Internet*. D.Sc. Dissertation, Hungarian Academy of Sciences (MTA) (2020).
6. Gyongyosi, L. Dynamics of entangled networks of the quantum internet. *Sci. Rep.*https://doi.org/10.1038/s41598-020-68498-x *(2020)*.
7. Gyongyosi, L. & Imre, S. Routing space exploration for scalable routing in the quantum internet. *Sci. Rep.*https://doi.org/10.1038/s41598-020-68354-y *(2020)*.
8. Gyongyosi, L. & Imre, S. Entanglement concentration service for the quantum internet. *Quantum Inf. Process.*https://doi.org/10.1007/s11128-020-02716-3 *(2020)*.
9. Gyongyosi, L. & Imre, S. Optimizing high-efficiency quantum memory with quantum machine learning for near-term quantum devices. *Sci. Rep.*https://doi.org/10.1038/s41598-019-56689-0 *(2020)*.
10. Gyongyosi, L. & Imre, S. Theory of noise-scaled stability bounds and entanglement rate maximization in the quantum internet. *Sci. Rep.*https://doi.org/10.1038/s41598-020-58200-6 *(2020)*.
11. Gyongyosi, L. & Imre, S. Entanglement accessibility measures for the quantum internet. *Quantum Inf. Process.*https://doi.org/10.1007/s11128-020-2605-y *(2020)*.
12. Gyongyosi, L. & Imre, S. Decentralized base-graph routing for the quantum internet. *Phys. Rev. A Am. Phys. Soc.*https://doi.org/10.1103/PhysRevA.98.022310 *(2018)*.
13. Gyongyosi, L. & Imre, S. Dynamic topology resilience for quantum networks. In *Proceedings of SPIE 10547*, Advances in Photonics of Quantum Computing, Memory, and Communication XI, 105470Z; https://doi.org/10.1117/12.2288707 (2018).
14. Gyongyosi, L. & Imre, S. Topology adaption for the quantum internet. *Quantum Inf. Process.*https://doi.org/10.1007/s11128-018-2064-x *(2018)*.
15. Gyongyosi, L. & Imre, S. Entanglement access control for the quantum internet. *Quantum Inf. Process.*https://doi.org/10.1007/s11128-019-2226-5 *(2019)*.
16. Gyongyosi, L. & Imre, S. Opportunistic entanglement distribution for the quantum internet. *Sci. Rep. Nat.*https://doi.org/10.1038/s41598-019-38495-w *(2019)*.
17. Gyongyosi, L. & Imre, S. Adaptive routing for quantum memory failures in the quantum internet. *Quantum Inf. Process.*https://doi.org/10.1007/s11128-018-2153-x *(2018)*.
18. Pirandola, S. & Braunstein, S. L. Unite to build a quantum internet. *Nature* **532**, 169–171 (2016).
19. Pirandola, S. End-to-end capacities of a quantum communication network. *Commun. Phys.* **2**, 51 (2019).
20. Wehner, S., Elkouss, D. & Hanson, R. Quantum internet: a vision for the road ahead. *Science* **362**, 6412 (2018).
21. Pirandola, S., Laurenza, R., Ottaviani, C. & Banchi, L. Fundamental limits of repeaterless quantum communications. *Nat. Commun.* **8**, 15043. https://doi.org/10.1038/ncomms15043 (2017).
22. Pirandola, S. *et al.* Theory of channel simulation and bounds for private communication. *Quantum Sci. Technol.* **3**, 035009 (2018).
23. Pirandola, S. Bounds for multi-end communication over quantum networks. *Quantum Sci. Technol.* **4**, 045006 (2019).
24. Pirandola, S. Capacities of repeater-assisted quantum communications. arXiv:1601.00966 (2016).
25. Pirandola, S. *et al.* Advances in quantum cryptography. *Adv. Opt. Photon.*https://doi.org/10.1364/AOP.361502 *(2020)*.
26. Laurenza, R. & Pirandola, S. General bounds for sender-receiver capacities in multipoint quantum communications. *Phys. Rev. A* **96**, 032318 (2017).
27. Gyongyosi, L. & Imre, S. Multilayer optimization for the quantum internet. *Sci Rep. Nat.*https://doi.org/10.1038/s41598-018-30957-x *(2018)*.
28. Gyongyosi, L. & Imre, S. Entanglement availability differentiation service for the quantum internet. *Sci. Rep. Nat.*https://doi.org/10.1038/s41598-018-28801-3 *(2018)*.
29. Gyongyosi, L. & Imre, S. Entanglement-gradient routing for quantum networks. *Sci. Rep. Nat.*https://doi.org/10.1038/s41598-017-14394-w *(2017)*.
30. Gyongyosi, L., Bacsardi, L. & Imre, S. A survey on quantum key distribution. *Infocom. J X* **I**(2), 14–21 (2019).

31. Preskill, J. Quantum computing in the NISQ era and beyond. *Quantum* **2**, 79 (2018).
32. Arute, F. *et al.* Quantum supremacy using a programmable superconducting processor. *Nature*https://doi.org/10.1038/s41586-019-1666-5 *(2019).*
33. Aaronson, S. & Chen, L. Complexity-theoretic foundations of quantum supremacy experiments. *Proceedings of the 32nd Computational Complexity Conference*, CCC '17, 22:1–22:67 (2017).
34. Harrow, A. W. & Montanaro, A. Quantum computational supremacy. *Nature* **549**, 203–209 (2017).
35. Foxen, B. *et al.* Demonstrating a continuous set of two-qubit gates for near-term quantum algorithms. *Phys. Rev. Lett.* **125**, 120504 (2020).
36. Harrigan, M. *et al. Quantum Approximate Optimization of Non-Planar Graph Problems on a Planar Superconducting Processor*. arXiv:2004.04197v1 (2020).
37. Rubin, N. *et al.* Hartree–Fock on a superconducting qubit quantum computer. *Science* **369**(6507), 1084–1089 (2020).
38. Arute, F. *et al. Observation of separated dynamics of charge and spin in the Fermi–Hubbard model*. arXiv:2010.07965 (2020).
39. Farhi, E., Goldstone, J. & Gutmann, S. *A Quantum Approximate Optimization Algorithm*. arXiv:1411.4028 (2014).
40. Farhi, E., Goldstone, J., Gutmann, S. & Neven, H. *Quantum Algorithms for Fixed Qubit Architectures*. arXiv:1703.06199v1 (2017).
41. Alexeev, Y. *et al. Quantum Computer Systems for Scientific Discovery*. arXiv:1912.07577 (2019).
42. Loncar, M. *et al. Development of Quantum InterConnects for Next-Generation Information Technologies*. arXiv:1912.06642 (2019).
43. Ajagekar, A., Humble, T. & You, F. Quantum computing based hybrid solution strategies for large-scale discrete-continuous optimization Problems. *Comput. Chem. Eng.* **132**, 106630 (2020).
44. Ajagekar, A. & You, F. Quantum computing for energy systems optimization: challenges and opportunities. *Energy* **179**, 76–89 (2019).
45. IBM. *A new way of thinking: The IBM quantum experience*. URL: http://www.research.ibm.com/quantum. (2017).
46. Farhi, E., Gamarnik, D. & Gutmann, S. *The Quantum Approximate Optimization Algorithm Needs to See the Whole Graph: A Typical Case*.arXiv:2004.09002v1 *(2020).*
47. Farhi, E., Gamarnik, D. & Gutmann, S. *The Quantum Approximate Optimization Algorithm Needs to See the Whole Graph: Worst Case Examples*. arXiv:arXiv:2005.08747 (2020).
48. Lloyd, S. *Quantum Approximate Optimization is Computationally Universal*. arXiv:1812.11075 (2018).
49. Sax, I. *et al.* Approximate approximation on a quantum annealer. *Proceedings of the 17th ACM International Conference on Computing Frontiers (CF 2020)* (2020).
50. Brown, K. A. & Roser, T. Towards storage rings as quantum computers. *Phys. Rev. Accel. Beams* **23**, 054701 (2020).
51. Gyongyosi, L. Quantum state optimization and computational pathway evaluation for gate-model quantum computers. *Sci. Rep.*https://doi.org/10.1038/s41598-020-61316-4 *(2020).*
52. Gyongyosi, L. & Imre, S. Dense quantum measurement theory. *Sci. Rep.*https://doi.org/10.1038/s41598-019-43250-2 *(2019).*
53. Gyongyosi, L. Objective function estimation for solving optimization problems in gate-model quantum computers. *Sci. Rep.*https://doi.org/10.1038/s41598-020-71007-9 *(2020).*
54. Gyongyosi, L. Decoherence dynamics estimation for superconducting gate-model quantum computers. *Quantum Inf. Process.*https://doi.org/10.1007/s11128-020-02863-7 *(2020).*
55. Gyongyosi, L. & Imre, S. Scalable distributed gate-model quantum computers. *Sci. Rep.*https://doi.org/10.1038/s41598-020-76728-5 *(2020).*
56. Gyongyosi, L. Unsupervised quantum gate control for gate-model quantum computers. *Sci. Rep.*https://doi.org/10.1038/s41598-020-67018-1 *(2020).*
57. Gyongyosi, L. Circuit depth reduction for gate-model quantum computers. *Sci. Rep.*https://doi.org/10.1038/s41598-020-67014-5 *(2020).*
58. Gyongyosi, L. & Imre, S. Quantum circuit design for objective function maximization in gate-model quantum computers. *Quantum Inf. Process.*https://doi.org/10.1007/s11128-019-2326-2 *(2019).*
59. Teplukhin, A., Kendrick, B. & Babikov, D. Solving complexeigenvalue problems on a quantum annealer with applications to quantumscattering resonances. *Phys. Chem. Chem. Phys.* https://doi.org/10.1039/D0CP04272B (2020).
60. Gill, S. S. *et al.* Quantum computing: A taxonomy, systematic review and future directions. *ACM Comput. Surv.* submitted (2020).
61. Caleffi, M. End-to-End Entanglement Rate: Toward a Quantum Route Metric, (2017) *IEEE Globecom*, https://doi.org/10.1109/GLOCOMW.2017.8269080 (2018).
62. Caleffi, M. Optimal routing for quantum networks. *IEEE Access*https://doi.org/10.1109/ACCESS.2017.2763325 *(2017).*
63. Caleffi, M. Cacciapuoti, A. S. & Bianchi, G. Quantum internet: from communication to distributed computing. In *NANOCOM '18: Proceedings of the 5th ACM International Conference on Nanoscale Computing and Communication* (2018).
64. Castelvecchi, D. The quantum internet has arrived. *Nature, News and Comment*. https://www.nature.com/articles/d41586-018-01835-3 (2018).
65. Cacciapuoti, A. S. *et al.* Quantum internet: networking challenges in distributed quantum computing. *IEEE Netw.*https://doi.org/10.1109/MNET.001.1900092 *(2018).*
66. Cuomo, D., Caleffi, M. & Cacciapuoti, A. S. Towards a distributed quantum computing ecosystem. https://digital-library.theiet.org/content/journals/10.1049/iet-qtc.2020.0002, https://doi.org/10.1049/iet-qtc.2020.0002 (2020).
67. Gyongyosi, L. & Imre, S. Training optimization for gate-model quantum neural networks. *Sci. Rep.*https://doi.org/10.1038/s41598-019-48892-w *(2019).*
68. Van Meter, R., Ladd, T. D., Munro, W. J. & Nemoto, K. System design for a long-line quantum repeater. *IEEE/ACM Trans. Netw.* **17**(3), 1002–1013 (2009).
69. Van Meter, R., Satoh, T., Ladd, T. D., Munro, W. J. & Nemoto, K. Path selection for quantum repeater networks. *Netw. Sci.* **3**(1–4), 82–95 (2013).
70. Pant, M. *et al.* Routing entanglement in the quantum internet. *npj Quantum Inf.* **5**, 25. https://doi.org/10.1038/s41534-019-0139-x (2019).
71. Chakraborty, K., Rozpedeky, F., Dahlbergz, A. & Wehner, S. Distributed routing in a quantum internet. arXiv:1907.11630v1 (2019).
72. Khatri, S., Matyas, C. T., Siddiqui, A. U. & Dowling, J. P. Practical figures of merit and thresholds for entanglement distribution in quantum networks. *Phys. Rev. Res.* **1**, 023032 (2019).
73. Khatri, S. Policies for elementary link generation in quantum networks. arXiv:2007.03193 (2020).
74. Kozlowski, W. & Wehner, S. Towards large-scale quantum networks. In *Proceedings of the Sixth Annual ACM International Conference on Nanoscale Computing and Communication*, Dublin, Ireland, arXiv:1909.08396 (2019).
75. Pathumsoot, P. *et al.* Modeling of measurement-based quantum network coding on IBMQ devices. *Phys. Rev. A* **101**, 052301 (2020).
76. Pal, S., Batra, P., Paterek, T. & Mahesh, T. S. Experimental localisation of quantum entanglement through monitored classical mediator. arXiv:1909.11030v1 (2019).
77. Miguel-Ramiro, J. & Dur, W. Delocalized information in quantum networks. *New J. Phys.*https://doi.org/10.1088/1367-2630/ab784d *(2020).*
78. Miguel-Ramiro, J., Pirker, A. & Dur, W. Genuine quantum networks: superposed tasks and addressing. arXiv:2005.00020v1 (2020).

79. Pirker, A. & Dur, W. A quantum network stack and protocols for reliable entanglement-based networks. *New J. Phys.* **21**, 033003. https://doi.org/10.1088/1367-2630/ab05f7 (2019).
80. Shannon, K., Towe, E. & Tonguz, O. On the Use of Quantum Entanglement in Secure Communications: A Survey. arXiv :2003.07907 (2020).
81. Amoretti, M. & Carretta, S. Entanglement verification in quantum networks with tampered nodes. *IEEE J. Sel. Areas Commun.*https://doi.org/10.1109/JSAC.2020.2967955 *(2020).*
82. Cao, Y. *et al.* Multi-tenant provisioning for quantum key distribution networks with heuristics and reinforcement learning: a comparative study. *IEEE Trans. Netw. Serv. Manag.*https://doi.org/10.1109/TNSM.2020.2964003 *(2020).*
83. Cao, Y. *et al.* Key as a service (KaaS) over quantum key distribution (QKD)-integrated optical networks. *IEEE Commun. Mag.*https://doi.org/10.1109/MCOM.2019.1701375 *(2019).*
84. Liu, Y. Preliminary Study of Connectivity for Quantum Key Distribution Network. arXiv:2004.11374v1 (2020).
85. Sun, F. Performance analysis of quantum channels. *Quantum Eng.*https://doi.org/10.1002/que2.35 *(2020).*
86. Chai, G. *et al.* Blind channel estimation for continuous-variable quantum key distribution. *Quantum Eng.*https://doi.org/10.1002/que2.37 *(2020).*
87. Ahmadzadegan, A. Learning to Utilize Correlated Auxiliary Classical or Quantum Noise. arXiv:2006.04863v1 (2020).
88. Bausch, J. Recurrent Quantum Neural Networks. arXiv:2006.14619v1 (2020).
89. Xin, T. Improved Quantum State Tomography for Superconducting Quantum Computing Systems, arXiv:2006.15872v1 (2020).
90. Dong, K. *et al.* Distributed subkey-relay-tree-based secure multicast scheme in quantum data center networks. *Opt. Eng.* **59**(6), 065102. https://doi.org/10.1117/1.OE.59.6.065102 (2020).
91. Amer, O., Krawec, W. O. & Wang, B. Efficient Routing for Quantum Key Distribution Networks. arXiv:2005.12404 (2020).
92. Krisnanda, T. *et al.* Probing quantum features of photosynthetic organisms. *npj Quantum Inf.* **4**, 60 (2018).
93. Krisnanda, T. *et al.* Revealing nonclassicality of inaccessible objects. *Phys. Rev. Lett.* **119**, 120402 (2017).
94. Krisnanda, T. *et al.* Observable quantum entanglement due to gravity. *npj Quantum Inf.* **6**, 12 (2020).
95. Krisnanda, T. *et al.* Detecting nondecomposability of time evolution via extreme gain of correlations. *Phys. Rev. A* **98**, 052321 (2018).
96. Krisnanda, T. Distribution of quantum entanglement: Principles and applications. Ph.D. Dissertation, Nanyang Technological University. arXiv:2003.08657 (2020).
97. Ghosh, S. *et al.* Universal quantum reservoir computing. arXiv:2003.09569 (2020).
98. Mewes, L. *et al.* Energy relaxation pathways between light-matter states revealed by coherent two-dimensional spectroscopy. *Commun. Phys.* **3**, 157 (2020).
99. Kopszak, P., Mozrzymas, M. & Studzinski, M. Positive maps from irreducibly covariant operators. *J. Phys. A Math. Theor.* **53**, 395306 (2020).
100. Guo, D. *et al.* Comprehensive high-speed reconciliation for continuous-variable quantum key distribution. *Quantum Inf. Process.* **19**, 320 (2020).
101. Chen, L. & Hu, M. Locally maximally mixed states. *Quantum Inf. Process.* **19**, 305 (2020).
102. Barbeau, M. *et al.* Capacity Requirements in Networks of Quantum Repeaters and Terminals. In *Proceedings of IEEE International Conference on Quantum Computing and Engineering (QCE 2020)* (2020).
103. Yin, J. *et al.* Entanglement-based secure quantum cryptography over 1,120 kilometres. *Nature* **582**, 501 (2020).
104. Santra, S. & Malinovsky, V. S. Quantum networking with short-range entanglement assistance. arXiv:2008.05553 (2020).
105. Komarova, K. *et al.* Quantum device emulates dynamics of two coupled oscillators. *J. Phys. Chem. Lett.*https://doi.org/10.1021/acs.jpclett.0c01880 *(2020).*
106. Gattuso, H. *et al.* Massively parallel classical logic via coherent dynamics of an ensemble of quantum systems with dispersion in size. *ChemRxiv*https://doi.org/10.26434/chemrxiv.12370538.v1 *(2020).*
107. Chessa, S. & Giovannetti, V. Multi-level amplitude damping channels: quantum capacity analysis. arXiv:2008.00477 (2020).
108. Pozzi, M. G. *et al.* Using Reinforcement Learning to Perform Qubit Routing in Quantum Compilers. arXiv:2007.15957 (2020).
109. Bartkiewicz, K. *et al.* Experimental kernel-based quantum machine learning in finite feature space. *Sci. Rep.* **10**, 12356. https://doi.org/10.1038/s41598-020-68911-5 (2020).
110. Kozlowski, W., Dahlberg, A. & Wehner, S. Designing a Quantum Network Protocol. arXiv:2010.02575 (2020).
111. Khan, T. M. & Robles-Kelly, A. A derivative-free method for quantum perceptron training in multi-layered neural networks. *ICONIP* **2020** (2020).
112. Mehic, M. *et al.* Quantum key distribution: a networking perspective. *ACM Comput. Surv.*https://doi.org/10.1145/3402192 *(2020).*
113. Kao, J. & Chou, C. Entangling capacities and the geometry of quantum operations. *Sci. Rep.* **10**, 15978. https://doi.org/10.1038/s41598-020-72881-z (2020).
114. Bae, J. *et al.* Quantum circuit optimization using quantum Karnaugh map. *Sci. Rep.* **10**, 15651. https://doi.org/10.1038/s41598-020-72469-7 (2020).
115. Bugu, S., Ozaydin, F. & Kodera, T. Surpassing the Classical Limit in Magic Square Game with Distant Quantum Dots Coupled to Optical Cavities. arXiv:2011.01490 (2020).
116. Welland, I. & Ferry, D. K. Wavepacket phase-space quantum Monte Carlo method. *J. Comput. Electron.*https://doi.org/10.1007/s10825-020-01602-6 *(2020).*
117. Ferguson, M. S., Zilberberg, O. & Blatter, G. Open quantum systems beyond Fermi's golden rule: Diagrammatic expansion of the steady-state time-convolutionless master equation. arXiv:2010.09838 (2020).
118. Villalba-Diez, J. & Zheng, X. Quantum strategic organizational design: alignment in industry 4.0 complex-networked cyber-physical lean management systems. *Sensors* **20**, 5856. https://doi.org/10.3390/s20205856 (2020).
119. Li, S. *et al.* Implementing Unitary Operators with Decomposition into Diagonal Matrices of Transform Domains. arXiv :2011.03250 (2020).
120. Xin, T. Improved quantum state tomography for the systems with XX+YY couplings and Z readouts. *Phys. Rev. A* **102**, 052410 (2020).
121. Pereg, U., Deppe, C. & Boche, H. Quantum Broadcast Channels with Cooperating Decoders: An Information-Theoretic Perspective on Quantum Repeaters. arXiv:2011.09233 (2020).
122. Gao, Y. L. *et al.* A novel quantum blockchain scheme base on quantum entanglement and DPoS. *Quantum Inf. Process.* **19**, 420. https://doi.org/10.1007/s11128-020-02915-y (2020).
123. Bacsardi, L. On the way to quantum-based satellite communication. *IEEE Commun. Mag.* **51**(08), 50–55 (2013).
124. Noelleke, C. *et al.* Efficient teleportation between remote single-atom quantum memories. *Phys. Rev. Lett.* **110**, 140403 (2013).
125. Kok, P. *et al.* Linear optical quantum computing with photonic qubits. *Rev. Mod. Phys.* **79**, 135–174 (2007).
126. Muralidharan, S., Kim, J., Lutkenhaus, N., Lukin, M. D. & Jiang, L. Ultrafast and fault-tolerant quantum communication across long distances. *Phys. Rev. Lett.* **112**, 250501 (2014).
127. Notzel, J. & DiAdamo, S. Entanglement-enhanced communication networks. In *IEEE International Conference on Quantum Computing and Engineering (QCE).* https://doi.org/10.1109/QCE49297.2020.00038 (2020).
128. Wereszczynski, K. *et al.* Cosine series quantum sampling method with applications in signal and image processing. arXiv :2011.12738v1 (2020).

129. Dai, W. *Quantum Networks: State Transmission and Network Operation*, PhD Dissertation, MIT (2020).
130. Qian, Z. & Tsui, C. Y. A Thermal Aware Routing Algorithm for Application-Specific Network-on-Chip. In: Palesi, M. and Daneshtalab, M. (Editors) *Routing Algorithms in Networks-on-Chip*, Springer, ISBN 978-1-4614-8273-4, ISBN 978-1-4614-8274-1 (eBook) (2014).
131. Palesi, M., Holsmark, R., Kumar, S. & Catania, V. Application specific routing algorithms for networks on chip. *IEEE Trans. Parallel Distrib. Syst.* **20**(3), 316–330 (2009).
132. Duato, J. A necessary and sufficient condition for deadlock-free adaptive routing in wormhole networks. *IEEE Trans. Parallel Distrib. Syst.* **6**(10), 1055–1067 (1995).
133. Tarjan, R. Depth-first search and linear graph algorithms. *SIAM J. Comput.* **1**(2), 146–160 (1972).
134. Chen, K. C., Chao, C. H., Lin, S. Y. & Wu, A. Y. Traffic- and Thermal-Aware Routing Algorithms for 3D Network-on-Chip (3D NoC) Systems. In: Palesi, M. and Daneshtalab, M. (Editors) *Routing Algorithms in Networks-on-Chip*, Springer, ISBN 978-1-4614-8273-4, ISBN 978-1-4614-8274-1 (eBook) (2014).
135. Zhang-Shen, R. & McKeown, N. Designing a predictable internet backbone with valiant load-balancing. In *Proceeding of Workshop of Quality of Service (IWQoS)* **2005** (2005).
136. Zhang-Shen, R. & McKeown, B. Designing a predictable internet backbone network. In *Third Workshop on Hot Topics in Networks* (HotNets-III) (2004).
137. Gyongyosi, L., Imre, S. & Nguyen, H. V. A survey on quantum channel capacities. *IEEE Commun. Surv. Tutor.*https://doi.org/10.1109/COMST.2017.2786748 *(2018).*
138. Van Meter, R. & Devitt, S. J. Local and distributed quantum computation. *IEEE Comput.* **49**(9), 31–42 (2016).
139. Rozpedek, F. *et al.* Optimizing practical entanglement distillation. *Phys. Rev. A* **97**, 062333 (2018).
140. Liao, S.-K. *et al.* Satellite-to-ground quantum key distribution. *Nature* **549**, 43–47 (2017).
141. Ren, J.-G. *et al.* Ground-to-satellite quantum teleportation. *Nature* **549**, 70–73 (2017).
142. Hensen, B. *et al.* Loophole-free Bell inequality violation using electron spins separated by 1.3 kilometres. *Nature* **526** (2015).
143. Hucul, D. *et al.* Modular entanglement of atomic qubits using photons and phonons. *Nat. Phys.* **11**(1) (2015).
144. Sangouard, N. *et al.* Quantum repeaters based on atomic ensembles and linear optics. *Rev. Mod. Phys.* **83**, 33 (2011).
145. Humphreys, P. *et al.* Deterministic delivery of remote entanglement on a quantum network. *Nature* **558** (2018).
146. Gyongyosi, L. & Imre, S. A survey on quantum computing technology. *Comput. Sci. Rev.*https://doi.org/10.1016/j.cosrev.2018.11.002 *(2018).*
147. Biamonte, J. *et al.* Quantum machine learning. *Nature* **549**, 195–202 (2017).
148. Lloyd, S., Mohseni, M. & Rebentrost, P. Quantum algorithms for supervised and unsupervised machine learning. arXiv:1307.0411 (2013).
149. Lloyd, S. & Weedbrook, C. Quantum generative adversarial learning. *Phys. Rev. Lett.* 121. arXiv:1804.09139 (2018).
150. Sheng, Y. B. & Zhou, L. Distributed secure quantum machine learning. *Sci. Bull.* **62**, 1019–1025 (2017).
151. Imre, S. & Gyongyosi, L. *Advanced Quantum Communications—An Engineering Approach* (Wiley-IEEE Press, New York, 2013).
152. Petz, D. *Quantum Information Theory and Quantum Statistics* Vol. 6 (Springer, Heidelberg, 2008).
153. Lloyd, S. Capacity of the noisy quantum channel. *Phys. Rev. A* **55**, 1613–1622 (1997).
154. Gisin, N. & Thew, R. Quantum communication. *Nat. Photon.* **1**, 165–171 (2007).
155. Leung, D., Oppenheim, J. & Winter, A. *IEEE Trans. Inf. Theory* **56**, 3478–90 (2010).
156. Quantum Internet Research Group (QIRG), web: https://datatracker.ietf.org/rg/qirg/about/(2018).
157. Chou, C. *et al.* Functional quantum nodes for entanglement distribution over scalable quantum networks. *Science* **316**(5829), 1316–1320 (2007).
158. Yuan, Z. *et al. Nature* **454**, 1098–1101 (2008).
159. Schoute, E., Mancinska, L., Islam, T., Kerenidis, I. & Wehner, S. Shortcuts to quantum network routing. arXiv:1610.05238 (2016).
160. Zhang, W. *et al.* Quantum secure direct communication with quantum memory. *Phys. Rev. Lett.* **118**, 220501 (2017).
161. Enk, S. J., Cirac, J. I. & Zoller, P. Photonic channels for quantum communication. *Science* **279**, 205–208 (1998).
162. Briegel, H. J., Dur, W., Cirac, J. I. & Zoller, P. Quantum repeaters: the role of imperfect local operations in quantum communication. *Phys. Rev. Lett.* **81**, 5932–5935 (1998).
163. Dur, W., Briegel, H. J., Cirac, J. I. & Zoller, P. Quantum repeaters based on entanglement purification. *Phys. Rev. A* **59**, 169–181 (1999).
164. Duan, L. M., Lukin, M. D., Cirac, J. I. & Zoller, P. Long-distance quantum communication with atomic ensembles and linear optics. *Nature* **414**, 413–418 (2001).
165. Van Loock, P. *et al.* Hybrid quantum repeater using bright coherent light. *Phys. Rev. Lett.* **96**, 240501 (2006).
166. Zhao, B., Chen, Z. B., Chen, Y. A., Schmiedmayer, J. & Pan, J. W. Robust creation of entanglement between remote memory qubits. *Phys. Rev. Lett.* **98**, 240502 (2007).
167. Goebel, A. M. *et al.* Multistage entanglement swapping. *Phys. Rev. Lett.* **101**, 080403 (2008).
168. Simon, C. *et al.* Quantum repeaters with photon pair sources and multimode memories. *Phys. Rev. Lett.* **98**, 190503 (2007).
169. Tittel, W. *et al.* Photon-echo quantum memory in solid state systems. *Laser Photon. Rev.* **4**, 244–267 (2009).
170. Sangouard, N., Dubessy, R. & Simon, C. Quantum repeaters based on single trapped ions. *Phys. Rev. A* **79**, 042340 (2009).
171. Dur, W. & Briegel, H. J. Entanglement purification and quantum error correction. *Rep. Prog. Phys* **70**, 1381–1424 (2007).
172. Lloyd, S., Mohseni, M. & Rebentrost, P. Quantum principal component analysis. *Nat. Phys.* **10**, 631 (2014).
173. Lloyd, S. The Universe as Quantum Computer, *A Computable Universe: Understanding and exploring Nature as computation*, Zenil, H. ed., World Scientific, Singapore. arXiv:1312.4455v1 (2013).
174. Shor, P. W. Scheme for reducing decoherence in quantum computer memory. *Phys. Rev. A* **52**, R2493–R2496 (1995).
175. Kobayashi, H., Le Gall, F., Nishimura, H. & Rotteler, M. General scheme for perfect quantum network coding with free classical communication, *Lecture Notes in Computer Science* (Automata, Languages and Programming SE-52 vol. 5555, Springer) 622–633 (2009).
176. Hayashi, M. Prior entanglement between senders enables perfect quantum network coding with modification. *Phys. Rev. A* **76**, 040301(R) (2007).
177. Hayashi, M., Iwama, K., Nishimura, H., Raymond, R. & Yamashita, S, Quantum network coding, *Lecture Notes in Computer Science* (STACS 2007 SE52 vol. 4393) ed Thomas, W. and Weil, P. (Berlin Heidelberg: Springer) (2007).
178. Kobayashi, H., Le Gall, F., Nishimura, H. & Rotteler, M. Perfect quantum network communication protocol based on classical network coding, *Proceedings of 2010 IEEE International Symposium on Information Theory* (ISIT) 2686-90. (2010).
179. Chen, L. & Hayashi, M. Multicopy and stochastic transformation of multipartite pure states. *Phys. Rev. A* **83**(2), 022331 (2011).
180. Xiao, Y. F. & Gong, Q. Optical microcavity: from fundamental physics to functional photonics devices. *Sci. Bull.* **61**, 185–186 (2016).
181. Mitzenmacher, N. & Upfal, E. *Probability and Computing: Randomized Algorithms and Probabilistic Analysis* (Cambridge University Press, Cambridge, 2005).

Acknowledgements
Open access funding provided by Budapest University of Technology and Economics (BME). The research reported in this paper has been supported by the Hungarian Academy of Sciences (MTA Premium Postdoctoral Research Program 2019), by the National Research, Development and Innovation Fund (TUDFO/51757/2019-ITM, Thematic Excellence Program), by the National Research Development and Innovation Office of Hungary (Project No. 2017-1.2.1-NKP-2017-00001), by the Hungarian Scientific Research Fund - OTKA K-112125, in part by the BME Artificial Intelligence FIKP grant of EMMI (Budapest University of Technology, BME FIKP-MI/SC), and by the Ministry of Innovation and Technology and the National Research, Development and Innovation Office within the Quantum Information National Laboratory of Hungary.

Author contributions
L.G.Y. designed the protocol and wrote the manuscript. L.G.Y. and S.I. and analyzed the results.

Competing interests
The authors declare no competing interests.

Additional information
Supplementary information is available for this paper at https://doi.org/10.1038/s41598-020-78960-5.

Correspondence and requests for materials should be addressed to L.G.

Reprints and permissions information is available at www.nature.com/reprints.

Publisher's note Springer Nature remains neutral with regard to jurisdictional claims in published maps and institutional affiliations.